AN ABSTRACT OF THE THESIS OF

Homero Cabrera-Muro for the degree of Master of Science

in Oceanography presented on August 20, 1976

Title: PRECISE NORTH-SOUTH OCEANOGRAPHIC TRANSECT IN THE PACIFIC OCEAN

Abstract approved: Redacted for privacy

Dr. P. Kilho Park

The Geochemical Ocean Sections Study (GEOSECS) program has carried out an intensive study of physical and chemical parameters in the Pacific and Atlantic Ocean. As a result, an enormous collection of high quality data has been amassed for these two oceans. To analyze the Pacific data, fourteen stations extending from about 50°N to 69°S near 180°longitude have been selected for this study. The section chosen provides a good continuous north-south section in the Pacific from near the Bering Sea to the Antarctic.

To study this massive extent of the oceanic regime, three methods were adopted. The first was to estimate, using Defant's method, the approximate level of no motion throughout the section. Secondly, vertical section plots were contoured for various physical and chemical parameters to help identify and trace oceanographic features throughout the Pacific. Finally, calculations for stability were applied to each station in the section to evaluate the correlation between features of stability and those seen in the section plots.

The depth of the level of no motion showed strong variability in

the Pacific Ocean. Generally, deeper levels were found in the higher latitudes with shallowing towards the Equator. In the high southern latitudes, no level of least motion could be identified. This is consonant with the condition that the establishment of a level of no motion involves noticeable stratification of the water column. In high latitudes, the more nearly uniform distribution of density throughout the water column inhibits the formation of layers of high stability and stratified condition.

It is also noted that a good general agreement is found between the depths of the layer of no motion and the observed oxygen minimum in the GEOSECS section. This is especially apparent in midlatitudes where the transition layer between the North and South Intermediate Waters and the Pacific Deep Waters is the region of the oxygen minimum. In the layer of the oxygen minimum, biochemical depletion occurs and there is likely to be minimal replenishment by horizontal and vertical advection and diffusion. Therefore, it is suggested that the oxygen minimum layer is closely related to a region of minimal horizontal movement. The calculation of the level of no motion in the Pacific GEOSECS sections supports this hypothesis.

The large scale circulation in the Pacific Ocean is clearly pictured by the parameter section plots obtained from the Pacific GEOSECS expedition. The North Pacific and Antarctic Intermediate Waters are clearly defined from their origins to disappearance by low salinity and high nutrient levels. The extent of the Pacific Deep Water throughout the Pacific is seen. This large mass of relatively homogenous water can be seen from the South to the North Pacific.

As the water moves northward, a gradual increase in nutrients and decrease in oxygen occurs. A third water type seen in the South Pacific is Antarctic Bottom Water. Its intrusion into the South Pacific can be defined in terms of the 27.86 sigma theta surface or by such parameters as oxygen, silicate, and apparent oxygen utilization (AOU).

In an attempt to correlate the various features seen in the vertical sections, stability profiles were prepared for each station. The vertical stability profiles did not show any strong features other than shallow and intermediate stability maxima. Recent discussion concerning a "benthic front" associated with the Antarctic Bottom Water intrusion into the South Pacific Ocean is not supported by any stability feature. Gradients in certain physical and chemical parameters do occur but the density gradients maximum expected in a frontal zone is not seen.

Precise North-South Oceanographic Transect
in the Pacific Ocean

by

Homero Cabrera-Muro

A THESIS

submitted to

Oregon State University

in partial fulfillment of
the requirements for the
degree of

Master of Science

June 1977

APPROVED:

Redacted for privacy

Professor of Oceanography
in charge of major

Redacted for privacy

Dean of School of Oceanography

Redacted for privacy

Dean of Graduate School

Date thesis is presented August 20, 1976

Typed by Margie Wolski for Homero Cabrera-Muro

ACKNOWLEDGMENTS

I wish to express my gratitude to the Consejo Nacional de Ciencia y Technologia, Republic of Mexico for bestowing me the opportunity to expose myself to a variety of extremely rewarding experiences at the beautiful campus of Oregon State University.

Dr. William Quinn, and Dr. Ricardo Pytkowicz deserve special thanks for their suggestions regarding this work. My thanks are also extended to Dr. Louis I. Gordon, Dr. Harry Freund and Dr. Larry Slotta for their suggestions and interest in this project. I also thank my good friends Edward and Joyce Seifert for their ever understanding encouragement.

I particularly enjoyed my friendship with Clif Dahm and Kilho Park. They were kind and cheerful toward me. I learned a good deal from both of them in our works and trips together, that include the Drake Passage Oceanographic Expedition of 1975. Also I cherish many fond memories of our hearty beer-drinking conversations.

Finally, I am indebted to Mrs. Cheryl Schurg for her gracious and efficient help in drafting this thesis.

This work was supported by the National Science Foundation grants 6X-28167 and GA.-12113-.

A mis Padres,

a Mexico

TABLE OF CONTENTS

LIST OF FIGURES

PRECISE NORTH-SOUTH OCEANOGRAPHIC TRANSECT IN THE PACIFIC OCEAN

I. INTRODUCTION

Since early times the history of man through the different cultures has been strongly linked to the seas and oceans. The increasing necessities of the world population have driven men to look for new sources of energy, food, and other materials for their own use. As a result, a systematic research has been developed and applied to understand the dynamics of the marine environment.

Recently, during the International Decade of Ocean Exploration (1970-1980), an intensive study of the Pacific and Atlantic Oceans was carried out through the GEOSECS (Geochemical Ocean Section Study) Program. This is a cooperative effort among the institutions of oceanography of the United States and several other nations.

The GEOSECS Program was constructed around three basic principles: 1) high density sampling program, in both horizontal and vertical sections, 2) study of the transport of various tracers, and 3) measuring all analyzable chemical constituents which show significant vertical and horizontal variations in the sea. Thus, as a result of this program, an enormous amount of hydrographic and chemical data has been obtained.

Oregon State University has participated in this effort by providing the expertise for the nutrients (phosphate, nitrate and nitrite, and silicate) and organic carbon analyses. Data for the Atlantic and Pacific Ocean were intensively obtained since September 1969. They are of the highest quality presently available for most of the measured parameters.

This paper is a study of the level of no motion along the GEOSECS section in the Pacific Ocean. This section extends from 50°N to 69°S near 180° longitude.

Several authors have attempted to establish a level of no motion in the Pacific Ocean (Dodimead et al., 1963; Wright, 1970; Reid and Lynn, 1971). Differences in dynamic heights (Defant, 1941), stability of the water column (Reid and Lynn, 1971), and the oxygen minimum layer have been proposed, among others, for use in establishing this level.

The GEOSECS observations in the Pacific Ocean permit study of the level of no motion and its variability over a wide range of latitudes. The high quality of the GEOSECS observations also permits study of the oxygen minimum layer in the Pacific Ocean. Findings using the oxygen minimum layer can be compared with those from the Defant (1941) method, and those from a study of the stability of the water column. In addition, the principal water masses of the Pacific Ocean are clearly identified by using several other chemical parameters from the GEOSECS section. The Pacific Ocean has been described in general by Sverdrup, Johnson and Fleming (1942). The South Pacific has been described in more detail by Reid (1965, 1972), and Reid and Lonsdale (1973). The water masses, their properties, and movements in the South Pacific have been studied by using temperature, salinity and oxygen distributions (Stommel, 1964; Tart, 1963; and Craig et al., 1972).

The oceanography of the Antarctic is described in the Southern

Ocean Workbook (ISOS, 1974). The Antarctic Intermediate Water has been defined by Reid (1965) and Johnson (1972).

The North Atlantic and Weddell Sea have been recognized as the main sources for Pacific Deep Water. Additional water masses of the South Pacific Ocean are discussed in Sverdrup et al. (1942).

The South Pacific surface circulation is shown in Figure 1. The Peru-Chile Current lies along the eastern boundary. This current flows to the west near 10°-15°S and becomes part of the South Equatorial Current which flows westward across the Equatorial Pacific and then southward at the western boundary of the South Pacific. This latter current is the Australian Current which joins the Antarctic Circumpolar Current in the Southern Pacific and flows eastward (Sverdrup et al., 1942).

Recently, Masuzawa and Nagasaka (1975) made several transects through the Tropical and Equatorial regions along 137°E in 1969-1974. They observed the variations of temperature and salinity in the upper waters. Vertically, Cromwell (1953) and Wooster and Cromwell (1958) note vertical mixing in the upper layer by the homogeneous salinity, oxygen, and phosphate distributions in this layer. Montgomery (1954) defines the structure of the thermocline as almost a discontinuity layer due to the strong gradients in temperature, oxygen, and phosphate.

The classic picture of the Equatorial circulation involves the westward flowing north and south Equatorial currents driven by the northeast and southeast trade winds, respectively, the Equatorial countercurrent and the Equatorial undercurrent.

Due to the seasonal variations of the trade winds, some changes in position and strength are observed in the North and South Equatorial Currents. Also, the position and strength of the Equatorial countercurrent changes seasonally. Knauss (1971) points out that the South Equatorial Current is somewhat stronger than the North Equatorial Current. He also states that the South Equatorial Current and the countercurrent are stronger than the North Equatorial Current during the northern summer. Conversely, the North Equatorial current is stronger in northern winter.

The Equatorial countercurrent as described by Reid (1948) is an eastward flowing current that compensates for the warm water piled up in the Western Pacific Ocean by the trade winds. Sverdrup et al. (1943) placed the northern and southern boundaries of the countercurrent at about 10°N and 5°N, respectively. From the distribution of salinity, oxygen, and phosphate, a distinct transverse circulation appears to be superimposed upon the flow toward the east (Sverdrup et al., 1942). Ascending motion takes place at the northern boundary (10°N) of the countercurrent and descending motion at the southern boundary (5°N). Due to convergence and divergence, a sort of spiral path is established.

The subsurface eastward flow (the Cromwell Current) has been studied by Knauss (1960) by using direct current measurements along the Equator in the Central and Eastern Tropical Pacific. The current, as defined by the 25 cm/sec contour, appears to be symmetrical about the Equator. It is about 300 meters wide and 200 meters thick. It extends from 92°W to at least 150°W (Knauss, 1971).

In the North Pacific, intensive oceanographic investigations have been conducted. Tully and Dodimead (1957) characterized two large water masses -- the Subarctic and Subtropic Waters. Dodimead, Favorite, and Hirano (1963) identified the Subarctic boundary between these two water masses by a nearly vertical isohaline of 34.0‰ which extends from the surface to a depth of about 200 to 400 meters. North of the boundary, in the Subarctic region, the salinity is at a minimum at the surface and increases with depth. South of the boundary in the Subtropical region, the salinity is at a maximum at the surface and decreases to a distinct minimum at about 500 meters.

Park (1967) studied chemical parameters in a section near 170°W from 35°N to 50°N during a summer which further defined the Subarctic and Subtropic water masses. Sverdrup et al. (1942) mentioned two additional water masses, the Western and Eastern water masses. They show a clockwise circulation (Fig. 1.1).

From the distribution of temperature, salinity, and radioactive carbon, Knauss (1962) inferred the flow of the Pacific Deep Water. He concluded that all water below 2500 meters in the Pacific is from a single source in the south, with a predominantly northward flow. The return flow occurs in the upper layers as a result of rising water in the North Pacific.

The surface circulation relative to the 1000 meter depth in the extreme western Pacific consists of the saline Kuroshio Current moving northward along the Japanese Islands. The main flow turns back eastward at about 36°N. This water continues eastward as the North Pacific Current to about 150°W where it moves southward. Part

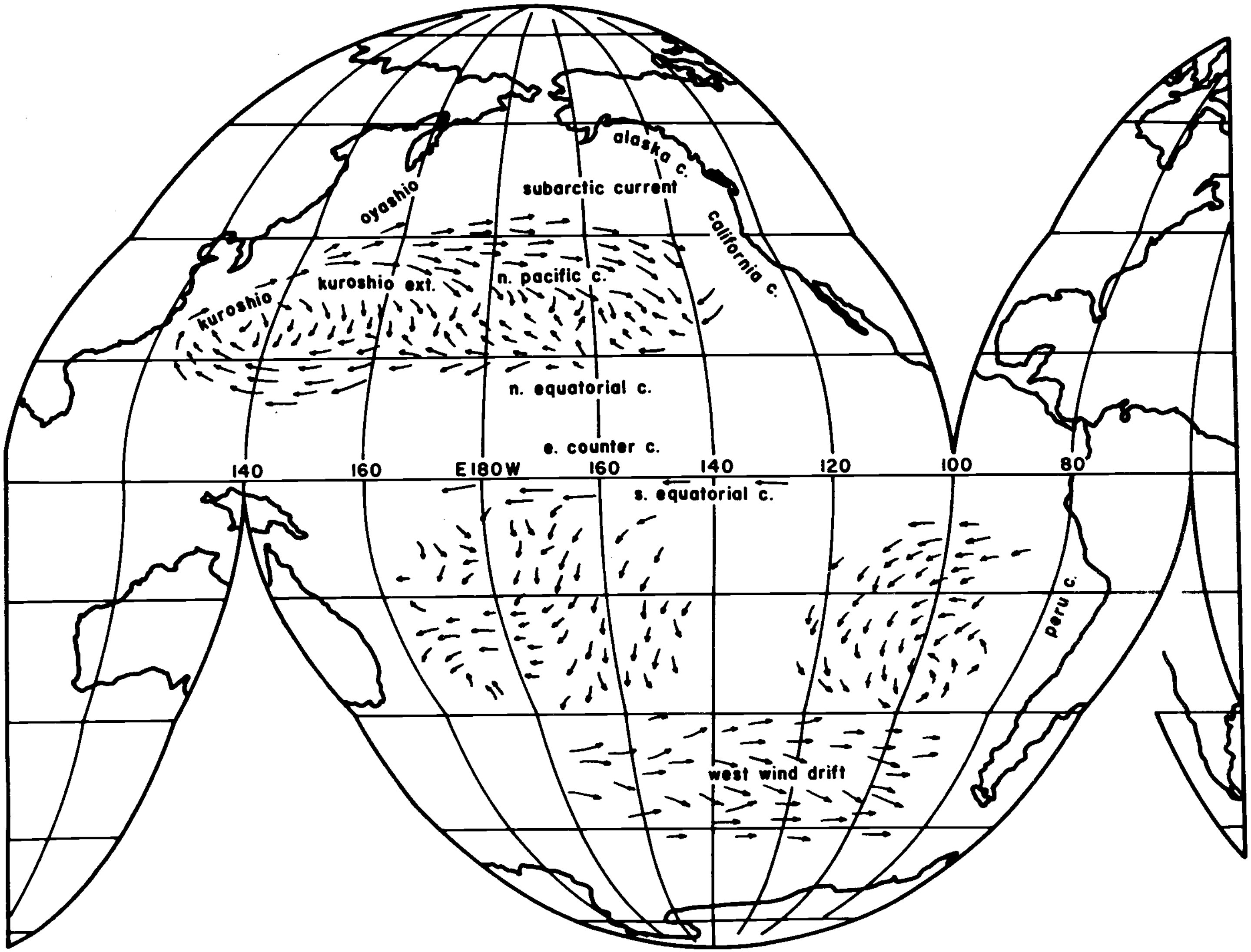

FIGURE I.I SURFACE CURRENTS IN THE PACIFIC OCEAN (FROM SVERDRUP ET AL. 1947) of the Kuroshio continues northeast to about 50°N where it meets the cold southward moving, less saline current, the Oyashio. This current is present along the eastern side of the Kuril and northern Japanese Islands. At the confluence of the two currents, extensive mixing occurs both horizontally and vertically. The mixed waters from the Kuroshio and Oyashio Currents continue eastward with the "West Wind Drift," or North Pacific Current, to approximately 300 miles form the Washington-Oregon coasts. Here the water divides, part turning south to form the California Current, and the rest flowing north into the Gulf of Alaska.

The part of the Oyashio Current in the northwest Pacific that does not actively mix with the Kuroshio Current moves northeastward to within 60 miles of the Aleutian Islands in the vicinity of 180°. Most of this water moves east as the Subarctic Current. It eventually flows into the Gulf of Alaska and around the Alaskan Gyre, making its return in the westward flowing Alaskan Current.

Other portions of the Oyashio form a gyre centered at about 50°N, 165°E. The water at the edge of the gyre mixes with the water of the Alaskan Current and moves westward to the end of the Aleutian Chain. A portion of this water enters the Bering Sea and some extends north into the Arctic Strait. The main branch forms a cyclonic circulation in the Bering Sea and flows southward along the Siberian coast. One part of this main branch becomes the East Kamchatka Current that flows to the south (Dodimead et al., 1963).

Although numerous studies have been carried out in the Pacific Ocean with reference to its chemical and physical oceanography, a detailed and rationalized study in this regard is still far from complete. One major problem has been the lack of a high quality consistent data set extending from the far north to the southermost extremes of the Pacific.

Therefore, it is proposed to study a north-south section of the Pacific by the use of the GEOSECS data, and to analyze the data from three different angles to view internal consistency and coherence. The first method will be to use the geostrophic approximation to calculate levels of least motion throughout the GEOSECS Pacific section. Secondly, the hydrographic data and chemical data will be presented in section plots and analyzed for consistency with past observations and the variation in the depths of the levels of no motion. Finally, a stability study will be done on the Pacific section to help in the identification of water masses and flow characteristics in the Pacific.

II. OBSERVATIONS AND METHODS

Since the inception of the GEOSECS Program, several calibration and testing stations or expeditions have been mounted in the Atlantic and Pacific Oceans. These include GEOSECS I, in the North Pacific; in September 1969, GOGO I and II, which were reoccupations of GEOSECS I in November 1971 and April 1972; and a leg of the SIO Antipode Expedition in the South Pacific which was carried out in August 1971. After successful completion of these stations, a systematic coverage of first the Atlantic and then the Pacific was begun.

From August 22, 1973 to April 8, 1974 the R/V MELVILLE of the Scripps Institution of Oceanography carried out a detailed survey of the Pacific Ocean. A high density sampling of physical and chemical parameters was obtained at a level of sophistication higher than any previous work in this area. From these stations, fourteen were selected to provide a representative north to south section. The station locations are shown in Figure 2.1.

A major reason for the strength of this hydrographic data set is due to a new conductivity-temperature-depth sensor of high sensitivity and response time, developed by Neil Brown at Woods Hole. With this instrument, temperature precisions of $\pm$ .002°C and conductivity precision translatable to $\pm$ .003‰ salinity were obtainable.

The nutrient data for the Pacific GEOSECS was taken with a modified AutoAnalyzer II system. Description of the methods and intercalibration tests were presented by Atlas et al. (1971), Hager et al. (1972) and Callaway et al. (1971). This data set gave

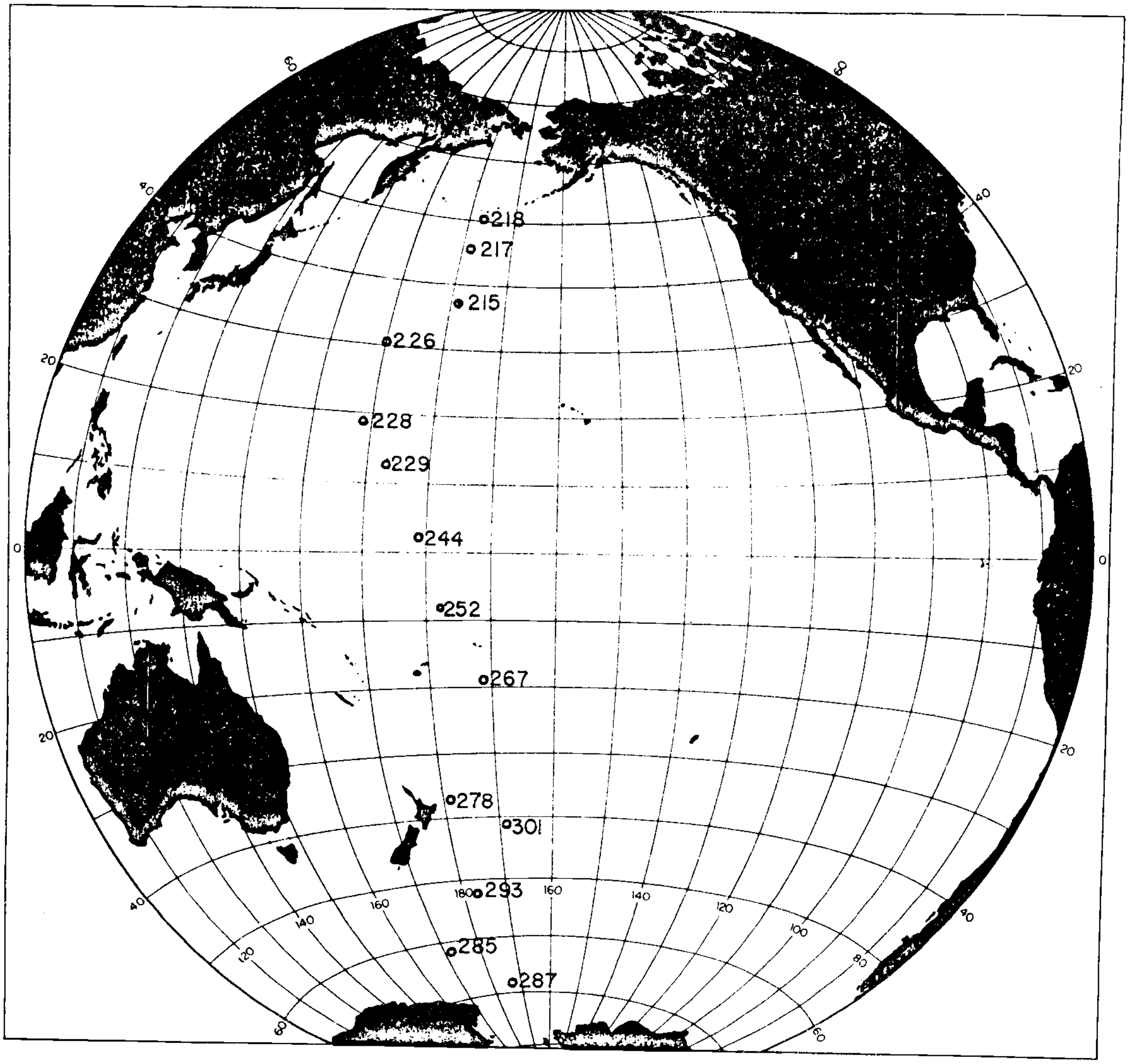

FIGURE 2.1 PACIFIC GEOSECS STATIONS USED FOR NORTH TO SOUTH SECTION IN THIS STUDY

precision better than 1% for all the analyses.

Oxygen, O_2, was measured by the Carpenter modification of the Winkler titration (Carpenter, 1965). Precision for O_2 was on the order of ± 1 μM/kg. All nutrient and O_2 values are expressed by μM/kg (micro-mole in a kilogram of seawater).

Preformed nutrients were calculated from the Redfield ratio (Redfield, Ketchum and Richards, 1963). For calculating apparent oxygen utilization, AOU, the saturation table for dissolved oxygen, O'_2, prepared by Gilbert, Pawley and Park (1968) was used.

III. LAYER OF NO MOTION ALONG THE PACIFIC OCEAN GEOSECS

The stations in the vertical profile of the GEOSECS track chosen for this study are shown in Figure 3.1. They extend from 50°N to 69°S at nearly the 180° longitude position. The quality of the data in this section makes it amenable for attempting to search for a level of no motion throughout the Pacific Ocean. Also, it is interesting to evaluate the best choice of depths of least motion along the section. An attempt is made here to reduce the arbitrariness in selecting this level by using the method of Defant (1941).

Under the assumption of non-accelerated, frictionless, irrotational fluid flow, the geostrophic currents are defined as those in which the pressure gradient force and the Coriolis force balance each other. The basic equation to calculate the geostrophic velocity between stations and across them is defined as:

$$(C_1 - C_2) = \left[\frac{\Delta D_A - \Delta D_B}{L \cdot f} \right] \qquad (3.1)$$

known as the Helland-Hanson formula (Sandstrom and Helland-Hanson, 1903). Where:

ΔD_A and ΔD_B = dynamic thickness of the same pressure interval

f = Coriolis parameter = $2\Omega \sin \phi$

L = distance between stations A, B

The geostrophic motions computed from the Helland-Hanson formula remain relative unless some valid observation is made to find a level where the motion can be assumed to be zero or otherwise known. In

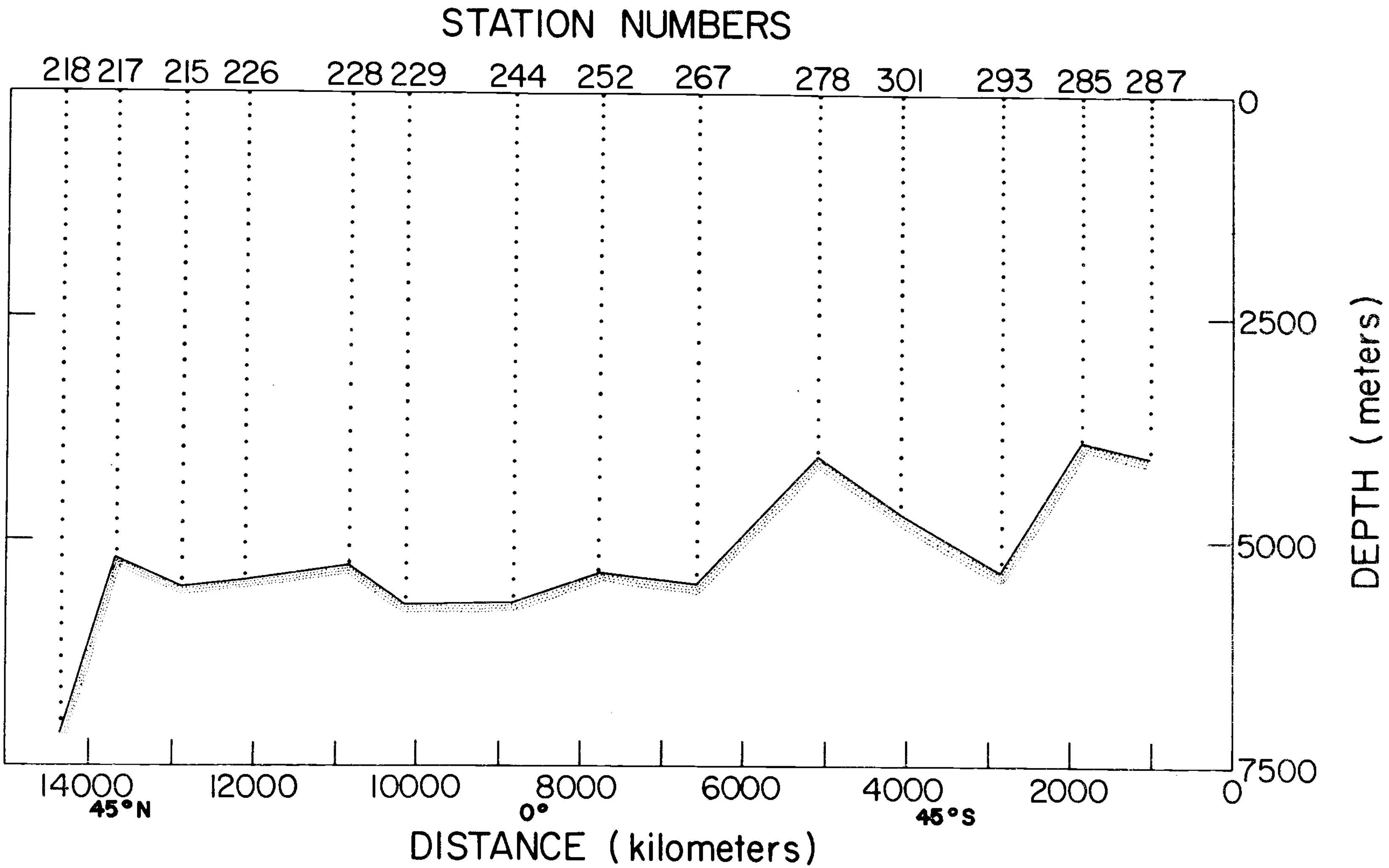

FIGURE 3.1 NORTH TO SOUTH VERTICAL TRANSECT OF THE GEOSECS STATIONS CHOSEN FOR THIS STUDY.

such a case, the field of relative geostrophic motion is calibrated and becomes an approximation of the actual velocity field.

Thus, the greatest problem in interpreting the geostrophic flow from the field of mass distribution is the choice of a reference surface. Since adequate current measurements for larger oceanic areas are not yet available to determine with sufficient accuracy the position of a zero layer or reference surface for dynamic computations, attempts have been made to find such a reference by indirect means. Some earlier investigators assumed the 'zero layer' reference level to be at the greatest depth, reasoning that the velocity decreases with depth and at great depths the isobaric surfaces are nearly horizontal. Although this crude approach may still give an adequate picture of the geostrophic currents at the surface, it may fail in those intermediate layers where the horizontal pressure gradient is weak.

In the case of nil horizontal pressure gradients between stations throughout the water column, a motionless layer may develop. The depth of this layer depends on the vertical density stratification. Therefore, a change of depth of the reference layer in different oceanic domains is to be expected.

A direct attempt to determine the depth of the layer of no horizontal motion was made by Defant (1941). He devised a scheme for determining the level of no motion between adjacent oceanographic stations by the consistency of differences in dynamic depths. It is suggested that a level of constant differences indicates a level of constant velocity or a level at which horizontal motion is small compared to that on the sea surface. Thus, Defant (1941) concludes that these deep layers with constant horizontal pressure gradients are motionless or nearly motionless, rather than at uniformity high speed as compared to the surface velocities.

To apply the Defant method (1941) along the GEOSECS Pacific section, a program was written that calculates the difference in dynamic thickness for the same pressure interval between stations. This difference is calculated repetitive for each depth of observation along the station sequence, assuming the sea surface to be level. The program also determines the mid-latitudes between stations. A detailed description of the program is given in Appendix I.

The vertical section plot of the level of least motion in the Pacific Ocean is shown in Figure 3.2 as determined by the Defant method. Also, the difference in dynamic heights versus depth is plotted in mid-latitudes between each pair of subsequent stations (Figs. 3.3a,b and c). The part of the curve which is drawn with a thicker line represents the depth at which the difference in dynamic heights are constant or almost constant. Special attention should be given to the curves at high latitudes, especially in the South Pacific Ocean. These curves seem to indicate that at these high latitudes in the South Pacific Ocean no layer of no motion can be found. This is due to the fact that a necessary condition for the establishment of a level of no motion is the stratification of the ocean. In these high latitudes the density is nearly uniform from the sea surface down to the bottom. Thus, all pressure gradients built up at the sea surface must be transmitted through all levels. Station combinations in latitudes greater than 50°S (Fig. 3.3e) support this expectation. Sometimes, the accuracy of the

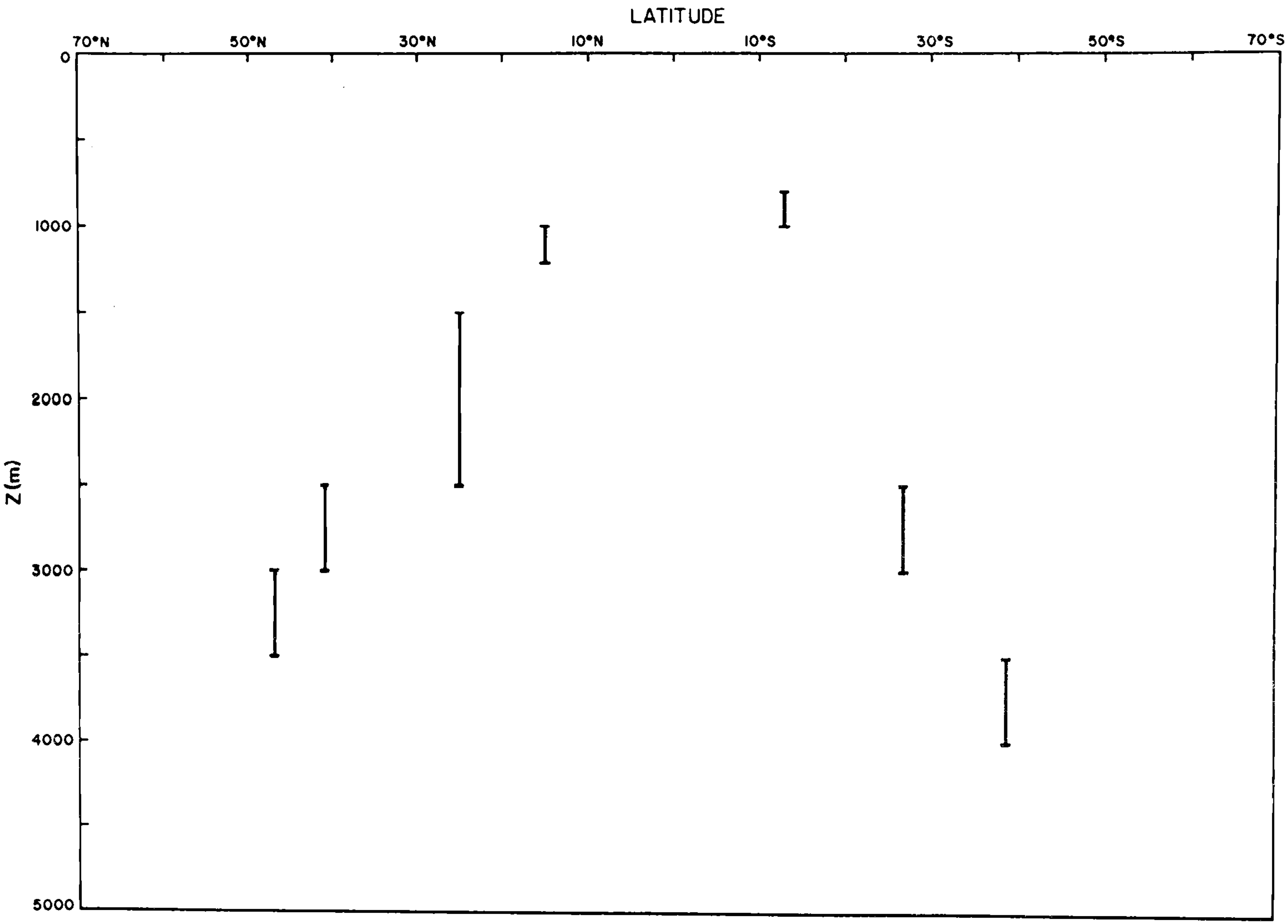

FIGURE 3.2 LEVEL OF NO MOTION FOR THE PACIFIC OCEAN

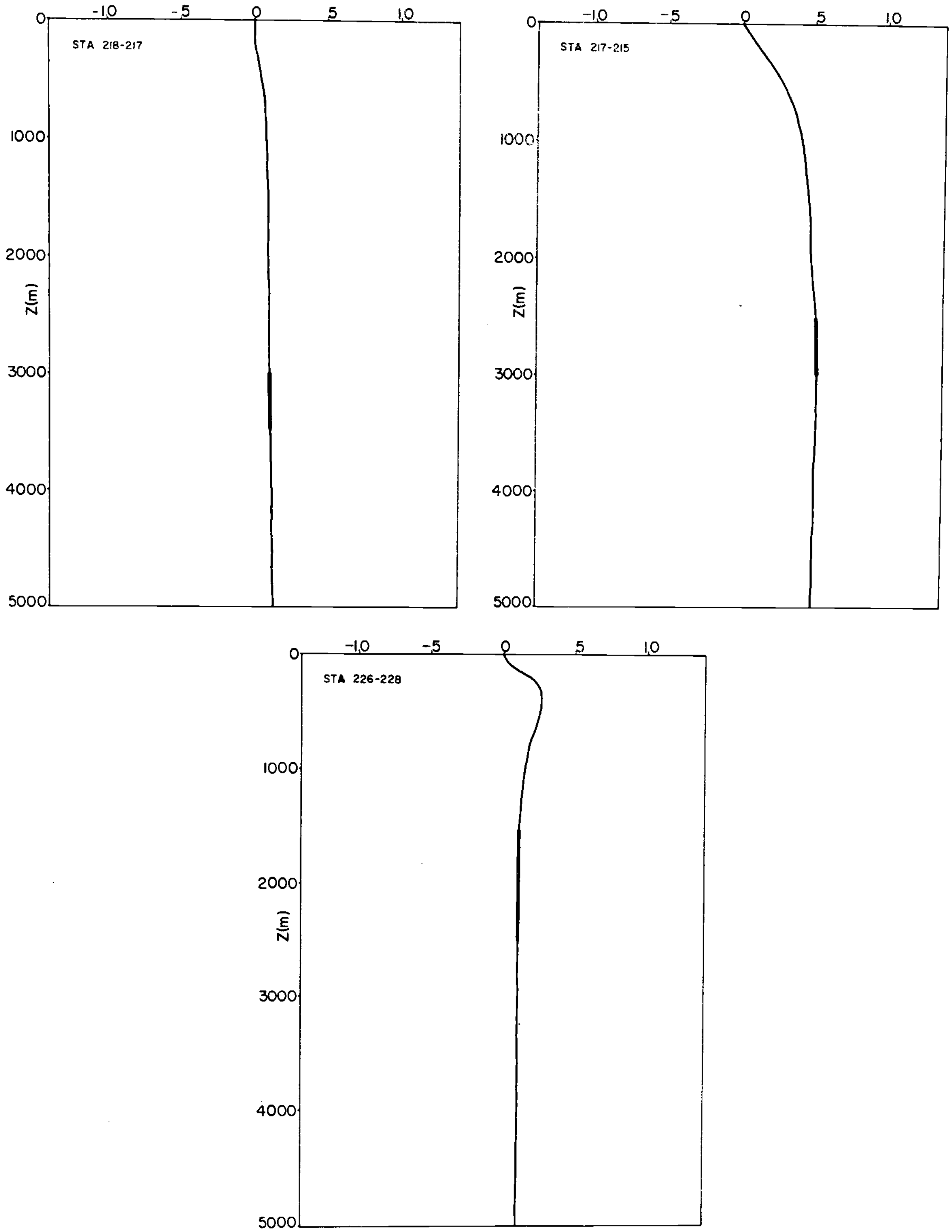

FIGURE 3.3a $(D_a - D_b)$ VS. Z(m) FOR PACIFIC GEOSECS STAS.

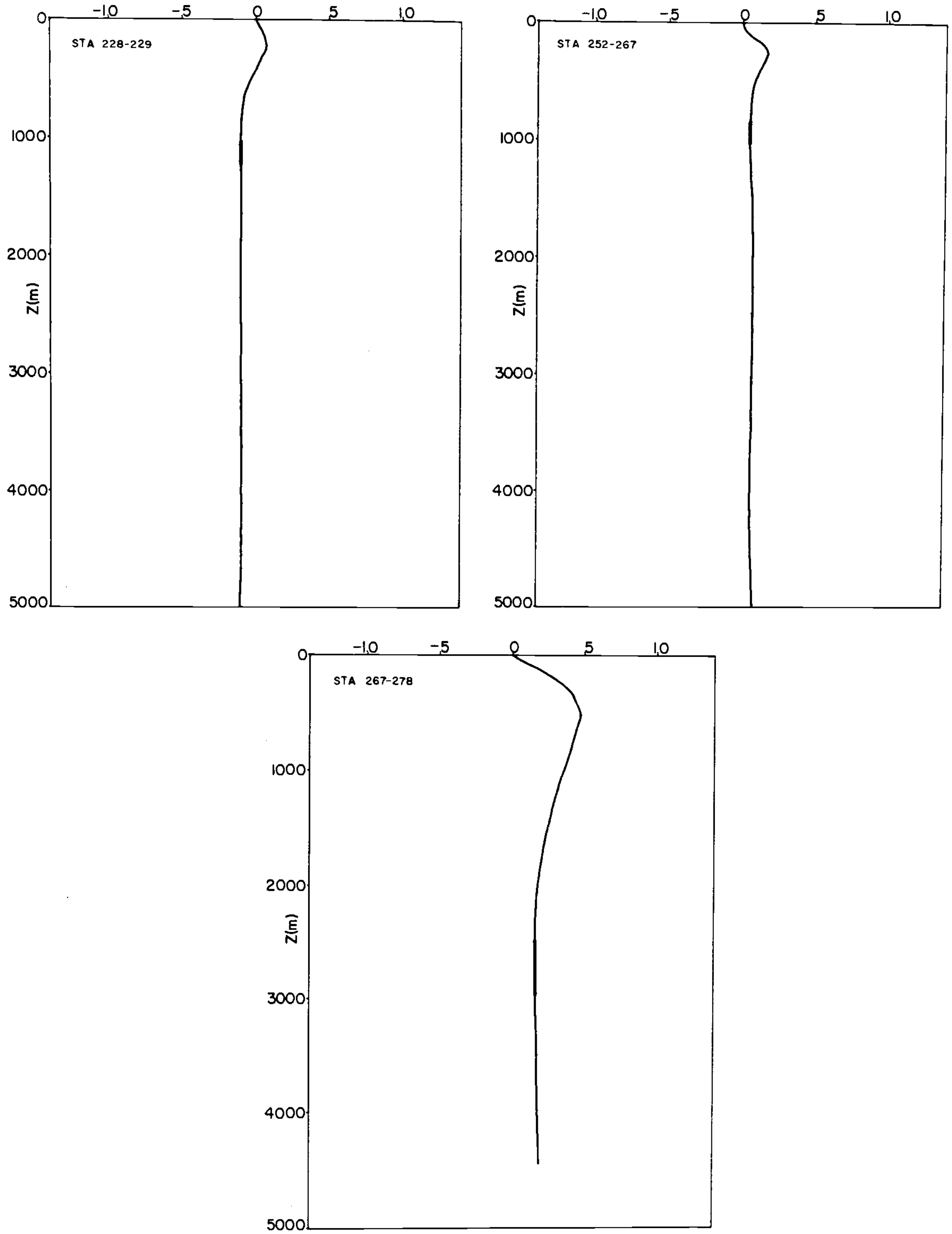

FIGURE 3.3b $(D_a - D_b)$ VS. FOR PACIFIC GEOSECS STAS.

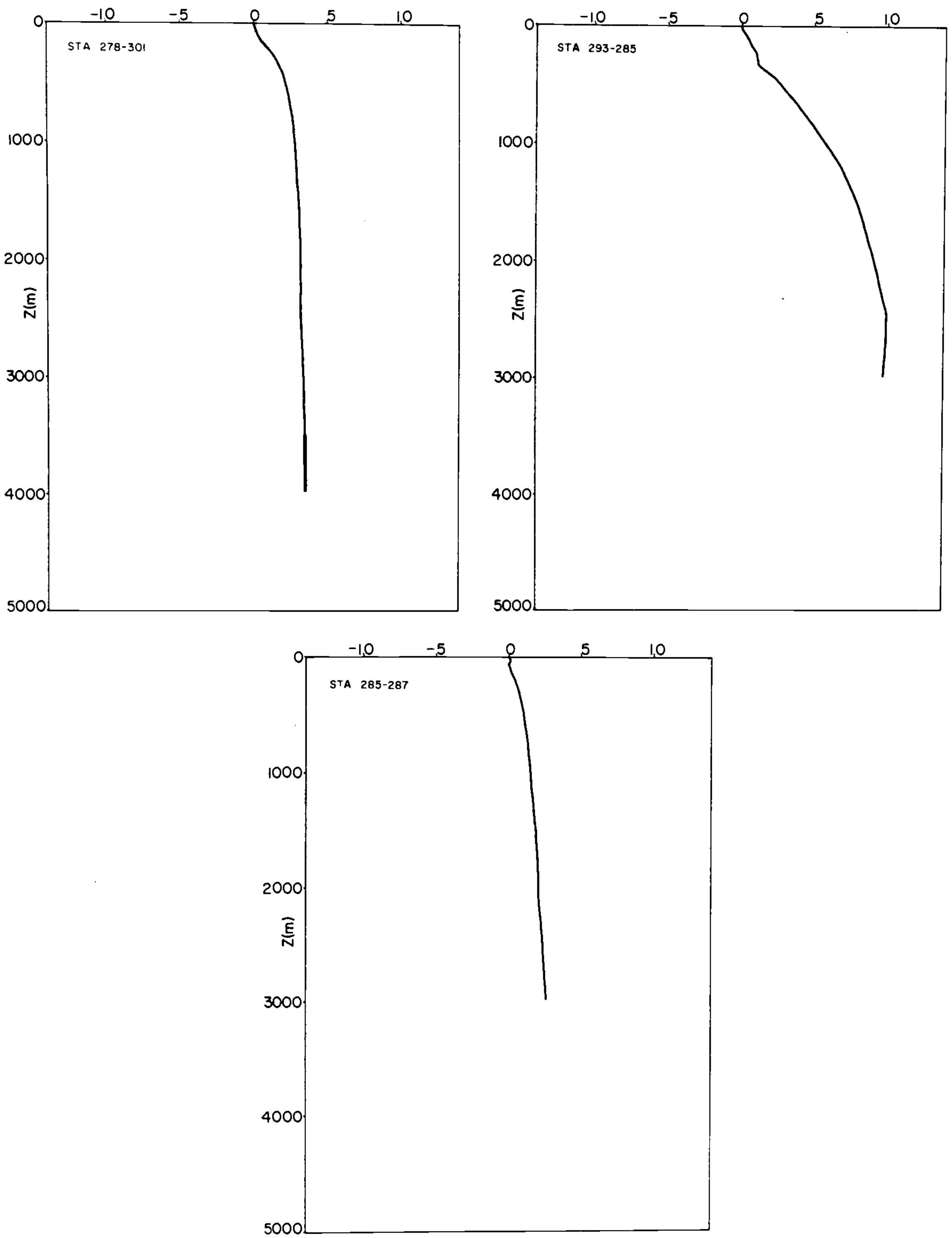

FIGURE 3.3c (D_a- D_b) VS Z(m) FOR PACIFIC GEOSECS STAS.

observations may not be sufficient to define the layer of least motion with confidence. Also, the asymmetrical distribution of some of the stations with respect to the longitudinal center of the section (180°) may cause some uncertainty when choosing the north to south level of no motion.

The range in depths for the layer of least motion throughout the GEOSECS section is shown in Figure 3.2. The distribution found here is similar to that proposed by Ostapoff (1957) for the Pacific Ocean. The depth range of the level of no motion slopes up from high latitudes toward the Equator. South of 50°S, no layer of equal horizontal pressure gradients was found. The lack of stratification throughout the water column inhibits the development of a layer of least motion. This is observed to a lesser extent in the northern latitudes. No calculations were made in a belt extending 15°N and south of the Equator due to the special conditions observed there.

An additional criterion to set the depth of the layer of no motion in the central parts of the ocean, where no strong vertical advection takes place, is suggested by Wyrtki (1962). In his classical paper on the oxygen minimum in relation to ocean circulation, Wyrtki (1962) presents a simple model to explain the mechanisms that form and maintain the layer of minimum oxygen in the oceans. He suggests that the ocean may be subdivided into three layers. The upper layer is well ventilated by its contact with the atmosphere and the oxygen content is maintained at a high level. The bottom layer is also of high oxygen content due to the effect of circualtion. He implies that, either the consumption of oxygen in this bottom layer is relatively small, or the circulation strong enough to maintain this high oxygen content. In addition, between these two layers exists a third water layer of minimum oxygen.

Depletion of oxygen is caused biochemically and replenishment occurs by horizontal advection. Therefore, the oxygen minimum layer is closely related to the layers of minimal horizontal movements. The model described above and the explanation given is suggested by Wyrtki (1962) to apply to the central parts of the oceans and to large scale features of the circulation. Also, he states that this explanation is not applicable to places where ocean currents extend as deep or deeper than the oxygen minimum layer. In this case the oxygen minimum will be simply carried with that particular current, and will have no significance with regard to the position of a motionless layer.

In the Pacific Ocean, the oxygen minimum layer shown in Figure 4.1c is associated with the Pacific Deep Water. Reid and Lynn (1971), and authors cited therein, suggest that the Pacific Deep Water results from the North Atlantic Deep Water, initially rich in oxygen, and deep waters formed in the Weddell Sea. In southern latitudes the North Atlantic waters are already somewhat depleted in oxygen when they meet the Weddell Sea Waters. On their movement toward the Pacific, they are additionally altered by the oxygen poor water of the northwest Indian Ocean. The resulting Pacific Deep Water extends northward into the Pacific Ocean. Nutrient data and AOU (Figs. 4.1c, e, f, g and h) suggest, as had been proposed Deacon (1937) and Reid et al. (1973), that the oxygen minimum then might be interpreted as a stratum of water returning southward from the North Pacific. There its oxygen has been even more depleted and its nutrients increased (Figs. 4.1c, e, f, g and h). Reid et al. (1973) and authors cited therein, also suggest that the southward extension of the oxygen minimum occurs in the region above the deep waters and beneath the intermediate waters. Sverdrup (1942) discusses this southward and upward flow as a compensation mechanism for the intermediate waters. The two main intermediate waters, the Antarctic Intermediate Waters (AAIW) and the North Pacific Intermediate Waters (NPIW), are created by mixing and sinking in the Arctic and Antarctic convergences, respectively. They flow north and south, toward the Equator, as a part of the anticyclonic gyres.

Warren (1973) has chosen 2000 meters depth as the depth of the level of no motion along 28°S. He based the choice partly upon the assumption that the oxygen minimum, which lies at about that level in the South Pacific for that latitude, represents a layer of minimum flow. Johnson (1971) in his Ph.D. thesis entitled "Antarctic Intermediate Water in the South Pacific Ocean" selects a depth of 2400 meters as a level of no motion to perform geostrophic calculations. He based this assumption on the depth of the flow reversal (or level of no motion) of the oxygen minimum layer.

In the North Pacific Ocean, Dodimead et al. (1963) studied the surface current regime applying the geostrophic method. A level of no motion was assumed to exist at 1000 meters depth. However, they recognized that this level may vary in some part of that region and recommended further studies of this problem.

Therefore, if the model of Wyrtki (1962) is compared with the level of no motion suggested by the data when using the Defant Method

(1941), especially in the central parts of the Pacific Ocean, a level of no motion such as that shown in Figure 3.2, can be assumed for east to west geostrophic transport calculations. This level is suggested to be the depth to which the anticylconic flow extends. Below this level at which the oxygen minimum occurs, the Pacific Deep Waters extend to the north. However, some departures of the oxygen minimum layer depth with respect to the proposed level of no motion are observed. The oxygen minimum tends to climb up over the level of no motion in lower and higher latitudes. In high latitudes, this might be due to a rain of organic material from the highly productive surface waters. The dead organic material sinks from the surface and is oxidized on its way down throughout the water column. As a result, oxygen below the euphotic zone is used in oxidation reactions and the oxygen minimum appears at less depth. Vertical diffusion may be taking place from the oxygen minimum to the warm and oxygen-poor waters above it in lower latitudes. This mechanism could then raise the oxygen minimum to the depths observed at Stations 228, 244 and 252 (Fig. 4.1c).

Another method for picking a level of no motion is based on the assumption that stability maxima separate opposite flowing waters (Wright, 1970; Reid and Lynn, 1971). It is assumed that a stability maximum represents a depth of minimum flow. In the Northeast Pacific, the circulation is such that the intermediate waters flow toward the Equator as a part of the anticylonic gyre and below the stability maximum. The deep waters are moving toward the north. From this information, a level of no motion can be inferred.

As it is shown later in this study, the analysis of the stability data along the GEOSECS Pacific section shows general features corresponding to the Intermediate and Pacific Bottom Waters but the level of no motion in the Pacific Ocean is not clearly defined by any density feature through the water column. However, the stability distribution is consonant with the lack of a level of no motion in high latitudes as it is pictured in Figure 3.2.

The suggested level of no motion cannot, of course, lead to invariant level. Aside from the uncertainty of this choice, the depth of the smallest differences can change in space and time as a result of other dynamical processes acting on the ocean.

IV. PARAMETER SECTION PLOTS

As mentioned earlier, the basic principles around which the GEOSECS program was constructed yield a high density sampling across the whole Pacific. From these data, vertical sections were constructed for different parameters from 50°N to 69°S at a longitude of 180° (Fig. 4). From these sections, correlations and variations can be made to the earlier proposition on the level of no motion.

Vertical sections of good quality data for conservative and non-conservative parameters are helpful to elucidate the source and extension of the different water masses observed in the Pacific Ocean. Conservative parameters such as salinity and temperature, cannot be altered by biological processes and, except at the boundaries, only advection and diffusion processes can account for changes in their values. Therefore, conservative parameters are a useful way to view the mixing processes between different water masses.

Non-conservative parameters, such as oxygen and the nutrients, are strongly affected by biochemical processes. Their distribution shows the amount to which the concentration has been changed once the waters have left their original source or sources. Changes in non-conservative concentrations are also related to AOU of the waters which can be used to calculate the conservative preformed nutrient quantities.

The vertical sections given in Figure 4.1 were found to be similar to those pictured by Redi (1965), and internally consistent with the concepts of deep-ocean circulation depicted by Stommel (1960).

Their consistency and precision also allows a more thorough and concise characterization of the circulation and distribution of these parameters in the Pacific.

To construct the GEOSECS Pacific section, fourteen stations were chosen. The section extends from 50°N to 69°S along about 180° longitude. The bottom bottle of each station goes nearly to the bottom. The bottom profiles were drawn by contouring these depths. The horizontal length of the section is 15000 km/∿8000 nautical miles. The depth is given in meters, and the maximum depth observed is about 7250 meters. The units used for oxygen, AOU, nutrients, and preformed nutrients are μM/kg. Salinity is given in parts per thousand (‰) and potential temperature in °C.

Potential Temperature:

Potential temperature distribution along the GEOSECS section in the Pacific Ocean is shown in Figure 4.1a. Surface values of this parameter show a decrease from near the Equator toward high latitudes. North Pacific and Antarctic Intermediate Water sources are well defined. A general decrease of temperature toward the bottom is observed in all latitudes. The Pacific Deep Water's complete extension from south to north is covered by the data. At southern latitudes, the low surface values are from the Antarctic Surface Waters which are present. At the bottom, in the South Pacific, rather cold water indicates the intrusion of Antarctic Bottom Waters.

The distribution of potential temperature yields similar results to the salinity and oxygen distributions. When coupled with salinity,

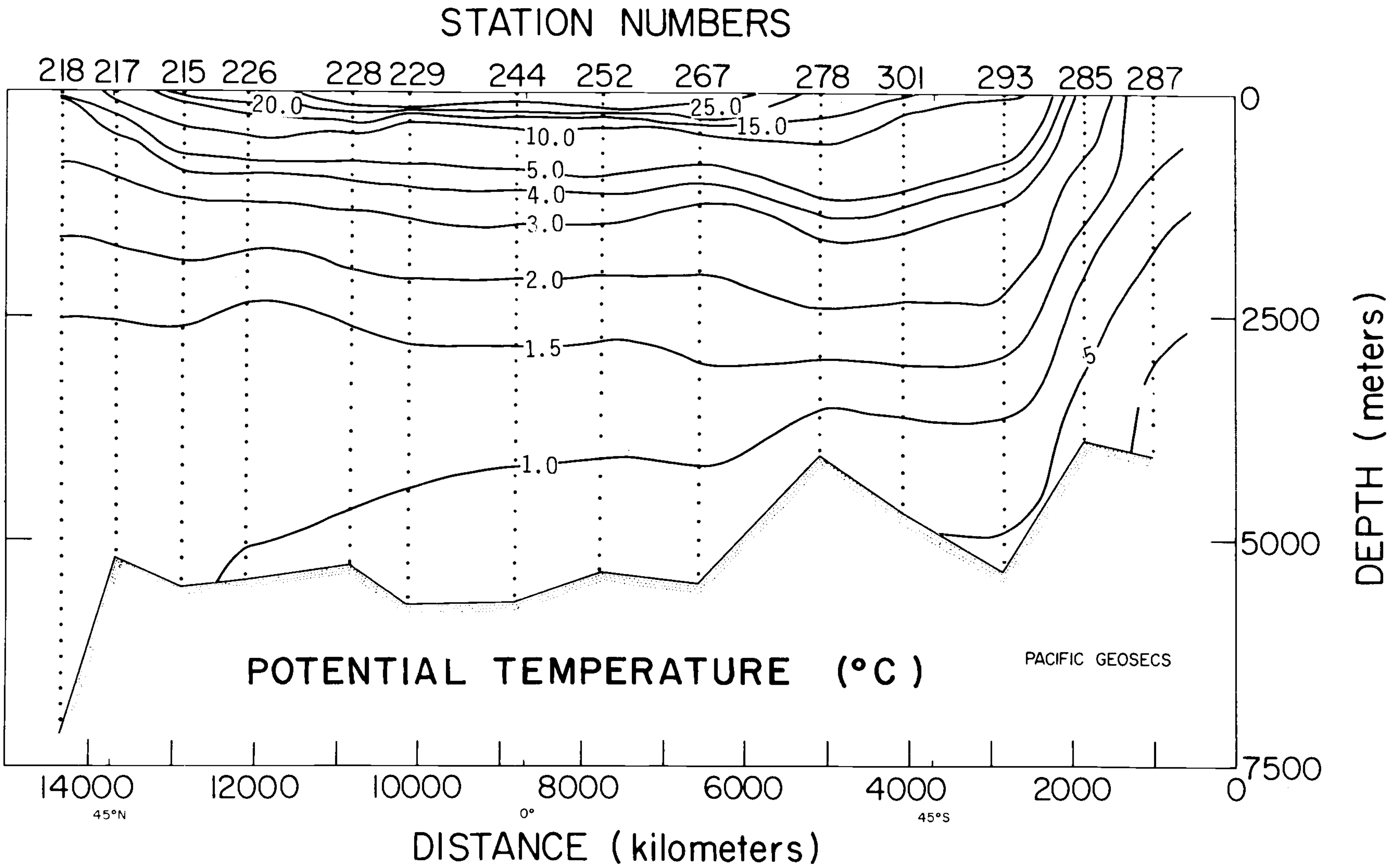

FIGURE 4.1a PACIFIC OCEAN SECTION, POTENTIAL TEMPERATURE

valuable information on stability can be obtained. This will be done in a later section.

Salinity:

The surface salinity of the Pacific Ocean has been concisely pictured recently by Reid (1973) and is observed in Figure 4.1b. First, two great cells of high salinity are found at the surface on either side of the Equator. These cells are roughly within the subtropical anticyclonic gyres. Lower surface salinities are observed at high latitudes and about the Equator. The salinity values for the haline cells are around 35.5‰ and 36.0‰ in the north and south Pacific, respectively. The low salinities in high latitudes are characterized by values of about 34.0‰.

This surface salinity distribution north to south in the Pacific Ocean is caused primarily by the differences in evaporation minus precipitation over the sea surface. Turbulent mixing and advection by currents also modifies the sea surface salinities (Neumann et al., 1966). The relationship between the meridional salinity distribution at the sea surface and the difference between evaporation minus precipitation was first studied by Wust (1936). He found that in all oceans the surface salinity has a minimum near the Equator and at high latitidues. This minimum is due to the excess of precipitation over evaporation. Maxima logically are reached in mid-latitudes where evaporation most greatly exceeds precipitation. The lower values observed in the southernmost latitudes are due to the heavy summer showers.

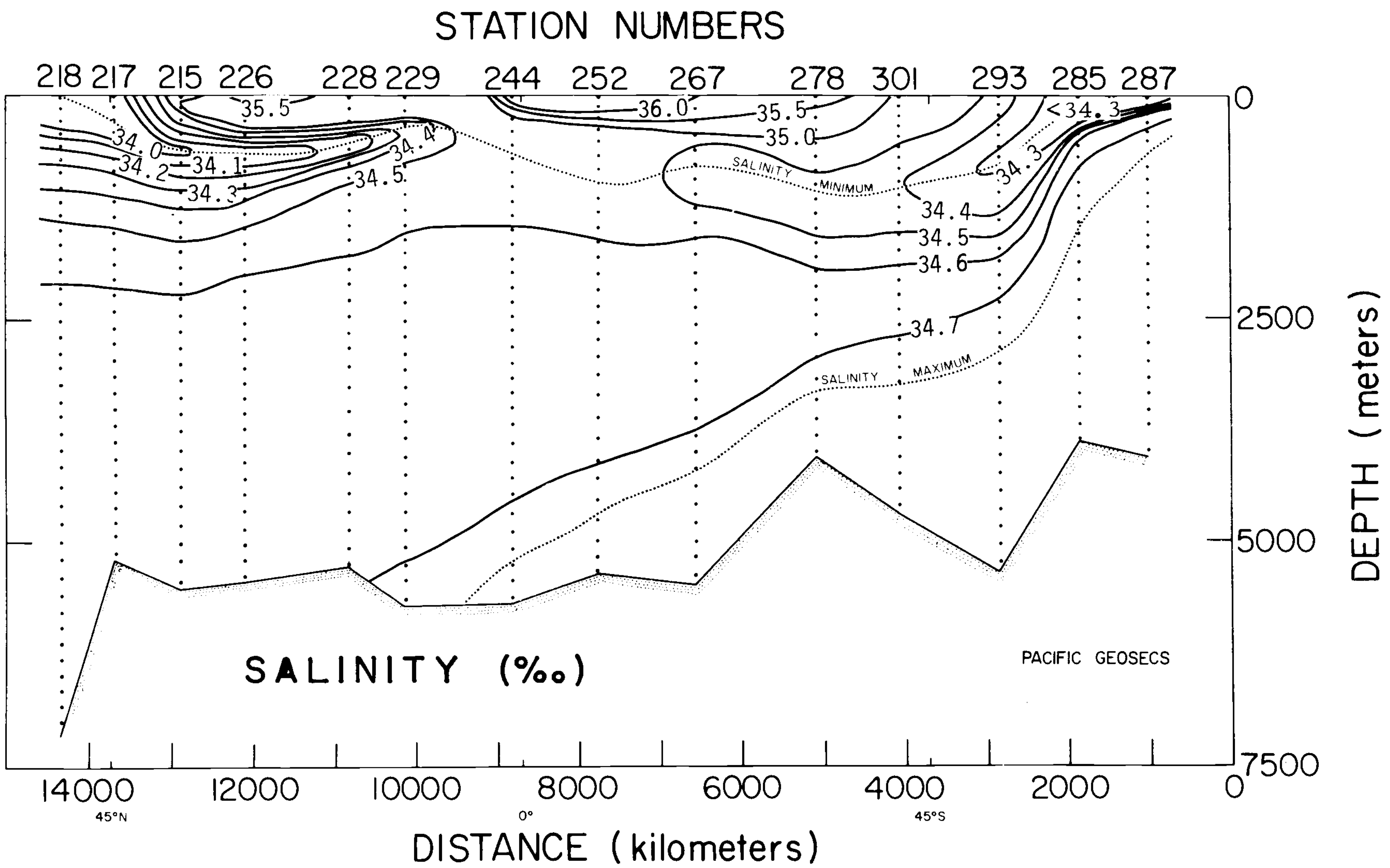

FIGURE 4.1b PACIFIC OCEAN SECTION, SALINITY

As suggested by Reid (1973), the high salinity cell of the South Pacific is not symmetric with that in the north. Not only is its salinity higher but it extends closer to the Equator than that of the north. Low surface salinity values are noted on the average at about 5°N (Wust, 1936). Masuzawa et al. (1975) placed the low salinity belt of Equatorial Surface Waters between 6°N and 13°N along 137°E in the western Pacific Ocean. They observed changes in salinity from year to year during five years of observations (1969-1974) and suggest that these noticeable changes are due to differences between years in precipitation and evaporation in the Equatorial region.

The shift in latitude of the surface salinity minimum is suggested to be a result of the seasonal variation in position and strength of the Equatorial Current System (Knauss, 1971). He states that the South Equatorial Current is stronger than the North Equatorial Current and that during the northern summer the South Equatorial Current moves further north while the North Equatorial Current is rather weak. During January, the North Equatorial Current is somewhat stronger than in July and it is closer to the Equator. As a result of this seasonal change in latitude of the current system, Reid (1972) suggests that the contribution of the high salinity waters from the North Pacific high cell to the Equatorial zone is less marked than that from the south.

Some other noticeable features appear in Figure 4.1b. They are the distinct salinity minimum and a deep salinity maximum. The salinity minima characterize the cores of two great tongues of low salinity water that extend toward the Equator from the surface in high latitudes. The tongue from the north is less saline and lies at shallower depths than that from the south. It is suggested by Reid (1965) that because of these salinity minima the water at intermediate depths in middle and low latitudes are lower in salinity than those above and below. Also he ascribes the source of the low salinity intermediate waters to the high latitude areas where high precipitation occurs.

The Antarctic Intermediate Waters are formed in the Antarctic convergence which lies in the South Pacific at 180° between about 50° and 60°S (Reid, 1965). There it is suggested that the Antarctic Surface Waters meet with the water north of the convergence and the resulting water sinks to intermediate depths. This water extends northward rich in oxygen, low in salinity and relatively cold in potential temperature.

The salinity minimum in the North Pacific locates the core of the North Pacific Intermediate Water. Its origin is not so clear as that in the south. Reid (1965) proposed that the North Pacific Intermediate Waters are formed in high latitudes by vertical mixing through the pycnocline. In addition, it is suggested that this mixing makes the waters in the pycnocline cold, low in salinity and rich in oxygen. These characteristics are transmitted Equatorward from gyre to gyre.

Near the Equatorial zone, where low surface salinity values are observed, the salinity minimum appears at less depth. Also, on both sides of the Equator some increase of salinity is observed within the salinity miminum. This change in lower latitudes may be due to conductivity and diffusivity processes rather than convective overturn.

Below the salinity minimum that charcterizes the intermediate waters, a fairly homogeneous water is observed in the Pacific Ocean with typical values of salinity of about 34.6 ‰. This water is the Pacific Deep Water. Its extent and ultimate origin have been thoroughly discussed by Reid et al. (1971). The Pacific Deep Water results from the lower North Atlantic water that meets the Antarctic waters and extends toward the east. It enters the Pacific Ocean south of New Zealand.

Below the Pacific Deep Waters, a salinity maximum is observed. The ultimate origin of this salinity maximum is to be found in the North Atlantic. Craig et al. (1972) attempted to show that the salinity maximum is also associated with a discontinuity surface termed a benthic front. He states that the existence of this front indicates spreading of the cold Antarctic Bottom Water into the Pacific Ocean. Chung (1975) also studied this feature and he states that in general it deepens northward along the western South Pacific and the salinity maximum remains until about 12°N where it vanishes on the bottom (Fig. 4.1b).

Sigma Theta, σ_θ :

Sigma theta or potential density is shown in Figure 4.1c. The Equatorial Waters are less dense than those at higher latitudes. The sources of intermediate and deep water formation are observed at high latitudes. A continuous increase in density values with depth is observed at all latitudes with no regions of high instability apparent. Pacific Deep Water is also well defined and the Antarctic Bottom Water

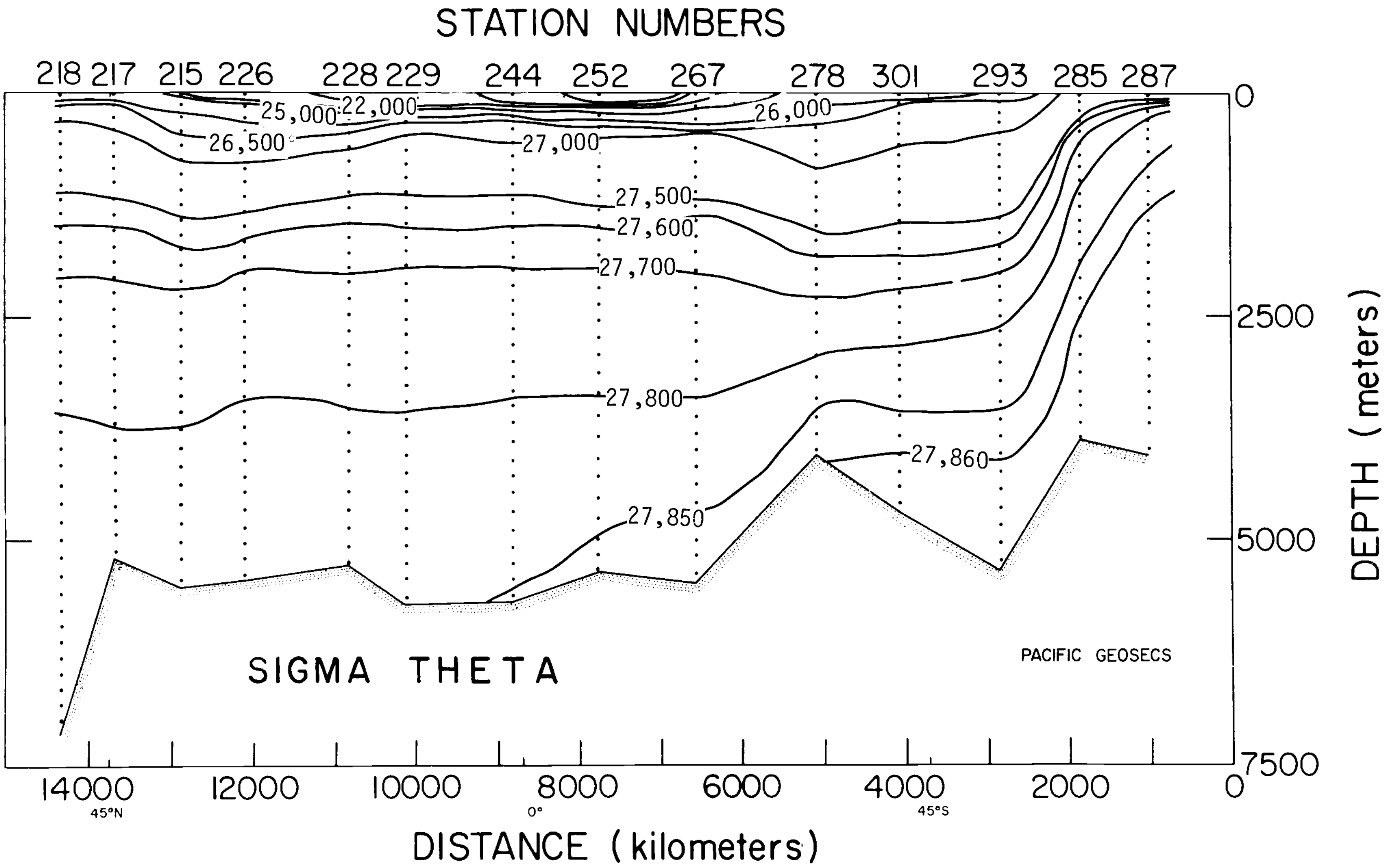

FIGURE 4.1c PACIFIC OCEAN SECTION, SIGMA THETA

intrusion in the South Pacific is defineable by the 27.85 σ_θ density contour.

Oxygen:

The oxygen field is more asymmetric about the Equator than the field of salinity (Fig. 4.1d). The near surface dissolved oxygen content exhibits the fact that surface temperature is the main control with increased temperature resulting in lower dissolved oxygen levels. The opposite extremes of two zones of high oxygen content are observed in high latitudes, where low temperatures occur, around the Arctic and Antarctic convergences.

One of the most striking features of the Pacific Ocean oxygen distribution is the tongue-like structure that extends from north to south. This tongue-like feature corresponds with an increase of oxygen content from north to south or an attenuation of a strong oxygen minimum moving southward. In general, the South Pacific Ocean shows higher oxygen concentrations than those observed in the North Pacific. Higher latitudes in the South Pacific show higher oxygen concentration than higher latitudes in the North Pacific. This increasing pattern south to north in oxygen concentration in the Pacific Ocean is related to the general south to north circulation of the Pacific Deep Water. Since the older waters have undergone more biochemical oxidation, there is a distinct correlation between oxygen content and age since the deep water was formed at the surface.

The oxygen minimum layer is the most noticeable feature in Figure 4.1c. This minimum has been discussed by several authors (Deacon,

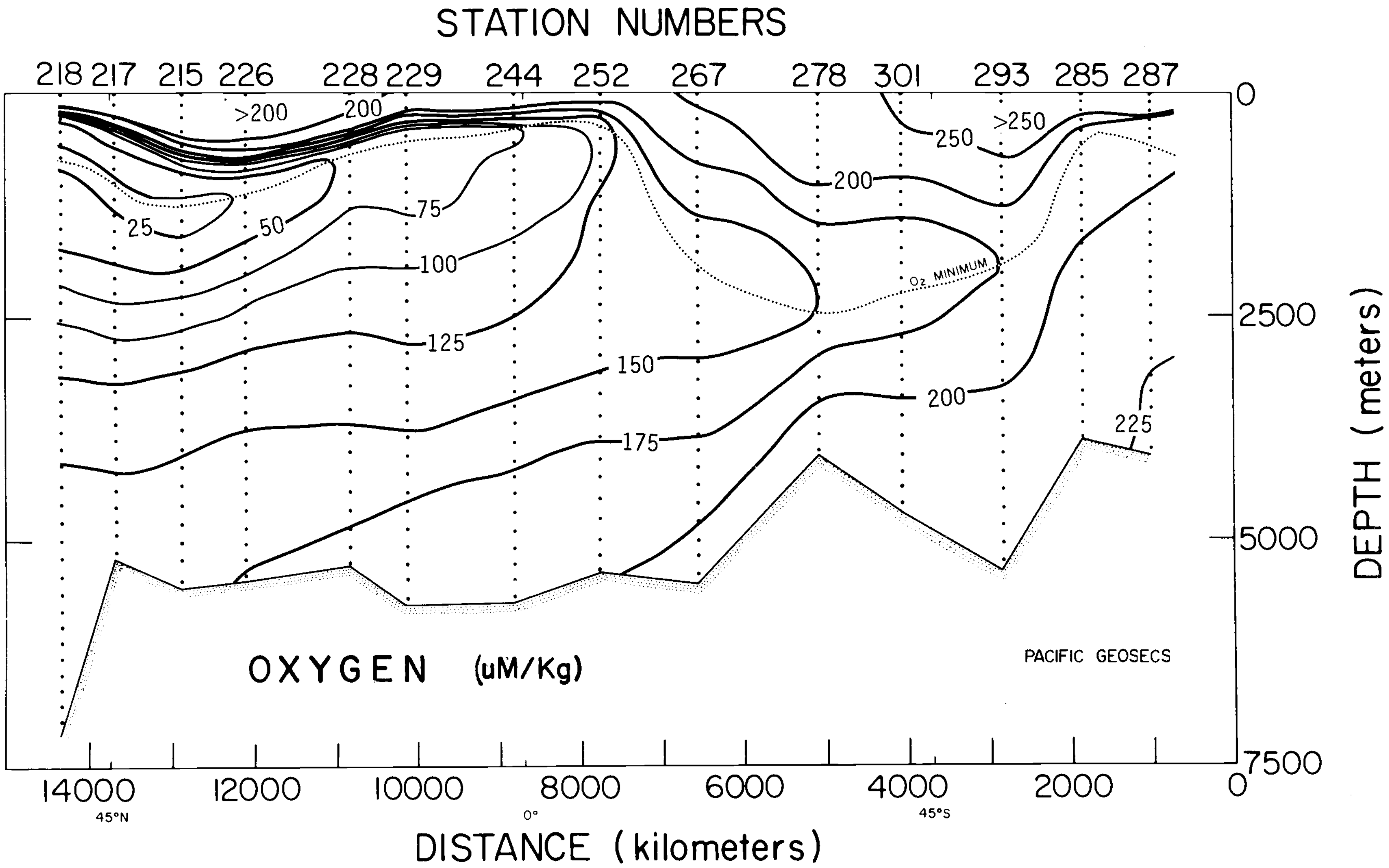

FIGURE 4.1d PACIFIC OCEAN SECTION, OXYGEN

1937; Sverdrup, 1942) and more recently by Craig et al. (1973). They suggest this minimum to be a southward flow of water with low oxygen content above the deep water and beneath the intermediate waters. In addition, Reid et al. (1973) proposed that this returning water from the North Pacific has been depleted in oxygen in northern latitudes by oxidation and its nutrients increased as its age increased. The oxygen minimum thus marks the transition zone between the oxygenated surface and intermediate waters and the Pacific Deep Waters.

This transition zone has been considered in different latitudes as a level of least motion between intermediate and deep waters by several authors (Dodimead et al., 1963; Johnson, 1971; Warren, 1973; Reid et al., 1973). Wyrtki (1963) in his extensive study of oceanic oxygen distributions states this explicitly.

The deep water oxygen concentration can be inferred by the deep circulation in the Pacific Ocean. All the water below 2500 meters in the Pacific is from a single source to the south. The flow is predominately northward and, therefore, the further north it is the older the age of this bottom water and the less oxygen it should contain. A return flow occurs in the upper layer as a result of rising water in the North Pacific. This return flow coupled with increased material for oxidation in the North Pacific most likely produces the distinct minimum discussed earlier.

The oxygen cross section at northern latitudes suggests that there is no significant addition of oxygen to the deep Pacific Ocean from the Arctic Ocean or the North Pacific Ocean. This may be associated with the presence of a stability maximum at about 800 to 900 meters depth in those latitudes. Therefore, Weyl (1965) suggests that all the oxygen for the Pacific Deep Water is supplied by inflow from the circum-Antarctic waters. The decrease in oxygen content downstream is due to oxidative processes and mixing with overlying, more poorly oxygenated waters.

The richer oxygenated waters in the south are obviously younger than those in the North Pacific and the isoxygen of 200 μM/kg defines well the extension of this rich oxygenated Antarctic Bottom Water. The oxygen concentration is attenuated northward until this feature vanishes on the bottom just south of the Equator. This characteristic narrowing is another visible feature of the so-called "benthic front" pictured by Chung (1975). Therefore, the "benthic front" may also be traced through the 200 μM/kg oxygen contour and gives some additional credence to the proposed frontal feature.

Phosphate:

Phosphate distribution in the Pacific Ocean is classically described by Reid (1962, 1965). Also, phosphate distribution in different zones of the Pacific Ocean have been studied by several authors (Park, 1967, 1968; Sogiura et al., 1965; Pytkowicz, 1966; Reid et al., 1973). General agreement is suggested by Reid (1962) between the maps of circulation and the phosphate content in the upper layers. This correspondence is observed in Figure 4.1e. High surface values are found at high latitudes (50°N, 60°S) and about the Equator. Divergence zones are proposed to account for the high phosphate content in the surface at these latitudes (Reid, 1962).

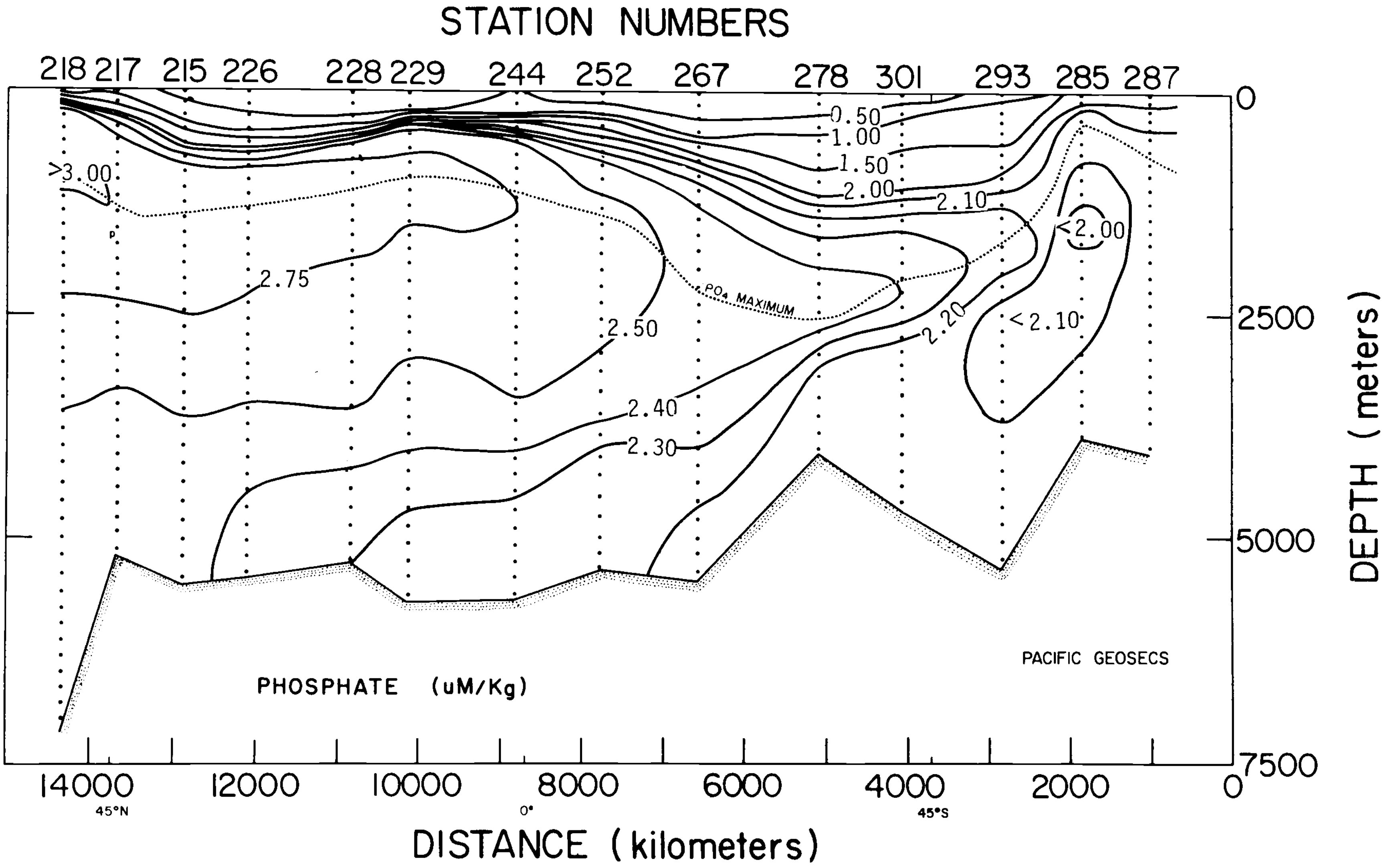

FIGURE 4.1e PACIFIC OCEAN SECTION, PHOSPHATE

In the Antarctic reaches of the South Pacific, Pytkowicz (1968) has proposed a returning intermediate water rich in nutrients at about 56° to 62°S to be the source for the rich surface water. He suggests that this southern intrusion of Antarctic Intermediate Water supplied nutrients to the highly productive Antarctic Surface Waters.

In the North Pacific Ocean, Park (1967, 1968) studied the Subarctic Boundary (40° to 50°N). He found a marked increase in the surface values of nutrient concentrations across the boundary from south to north. It is suggested that these high values near the Aleutian Trench may be a product of the upward divergence of the subsurface water.

Moving to the Equatorial region, the Equatorial divergence proposed by Sverdrup (1942) is suggested to account for the relatively high phosphate values nearer the surface. High surface values are not visible in Figure 4.1e but a bunching of the phosphate contours in the Equatorial zone is highly noticeable.

At middle latitudes, the low phosphate content at the surface is a product of the uptake by the phytoplankton and a reduced subsurface supply through the pycnocline. As with the other chemical nutrients, a sterile desert exists in these middle latitudes with respect to phosphate.

The phosphate maximum is seen at intermediate depths in the Pacific deepening south of the Equator to the Antarctic region. The phosphate maximum is located at about the same depths as the oxygen minimum. Along this surface, as well as in the deep water, where more regeneration of phosphate has taken place. The phosphate distribution also correlates well with the deep water circulation from south to north.

Finally, a core of low phosphate water is observed in the South Pacific. This zone may suggest the presence of waters of relatively low phosphate content of North Atlantic and Antarctic origin. This water being transported in the Antarctic Circumpolar Current has mixed with low phosphate North Atlantic Deep Water and still exhibits this lower phosphate concentration in the southern Pacific Ocean.

Nitrate:

Nitrate distribution that includes nitrite concentration shows the same north to south tongue-like distribution of other parameters (Fig. 4.1f). The same processes, i.e. synthesis, uptake, regeneration, and advection, that affect phosphate, determine the nitrate distribution. High surface values are explained in terms of divergence zones (Reid, 1962-1965). In addition, low surface values are suggested to be a product of poor subsurface replenishment and synthesis.

As with phosphate, productive zones are observed in high latitudes and about the Equator. Middle latitudes are characterized by low nitrate content at the surface. Nitrate distributions have been studied in the north and northeast Pacific Ocean by several authors (Park, 1967, 1968; Anderson et al., 1969).

In the northeast Pacific, Park (1967, 1968) observed a noticeable increase of surface values of nitrate content across the Arctic Boundary. He also suggests, as for other chemical features, that those high values may be due to divergence south of the Aleutian Arc.

The nitrate maximum is somewhat deeper than the phosphate maximum. This is due to the faster release of phosphorus from

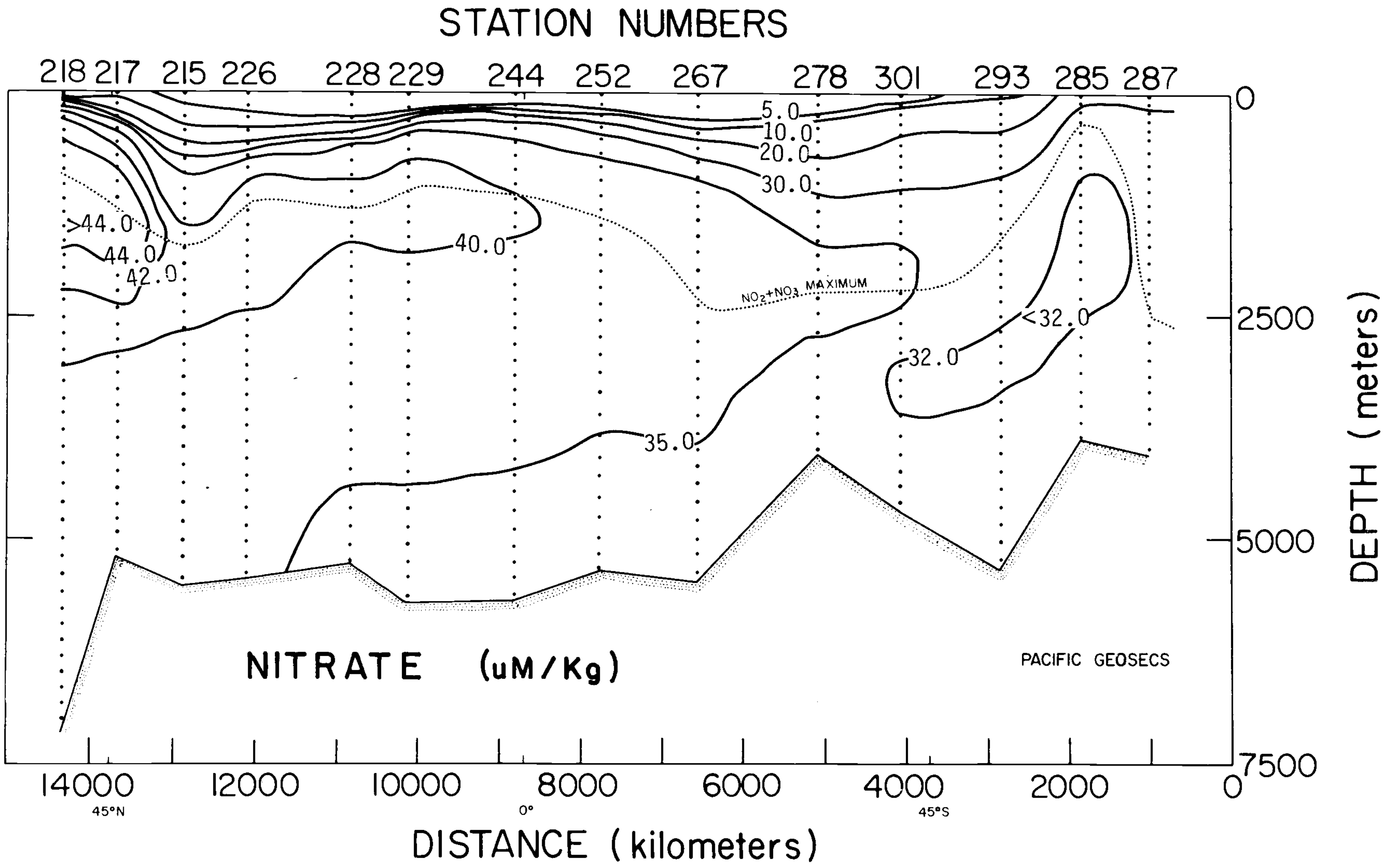

FIGURE 4.1f PACIFIC OCEAN SECTION, NITRATE

phytoplankton as they sink and the slower biochemical oxidation of nitrogen species to nitrate than phosphate. Nitrate distribution in deep waters is also consonant with the south to north circulation previously mentioned (Reid, 1965, 1971, 1973). Lower values of nitrate are observed in the younger southern waters. High values of nitrate are present in the older northern waters (Reid, 1965).

A core of relatively low nitrate content is present in southern latitudes. This low nitrate water again most likely originates in the North Atlantic as does the similar phosphate feature. The large difference in nutrient concentrations between the North Atlantic Deep Water (NADW) and Antarctic waters enables the effect of NADW to be seen throughout the world oceans.

Silicate:

The dissolved silicate along GEOSECS transect, shown in Figure 4.1g, resembles to some extent the north-south distribution of silicate in the Pacific Ocean illustrated in the book entitled Chemistry of the Pacific Ocean (Academy of Science, USSR, 1966). Bogoyavlenskiy (1967) also studied the dissolved silica and deep-sea sediments in the Pacific Ocean. He shows the distribution of dissolved silica from north to south (50°N-70°S) and found consistency with the principal water movements determined from other oceanographic parameters.

The silica content in the surface layer decreases from high latitudes towards the Equator. Except for the most southern and northern stations, silicate is at low levels. This is primarily due to the uptake of silica by organisms. This surface depletion clearly

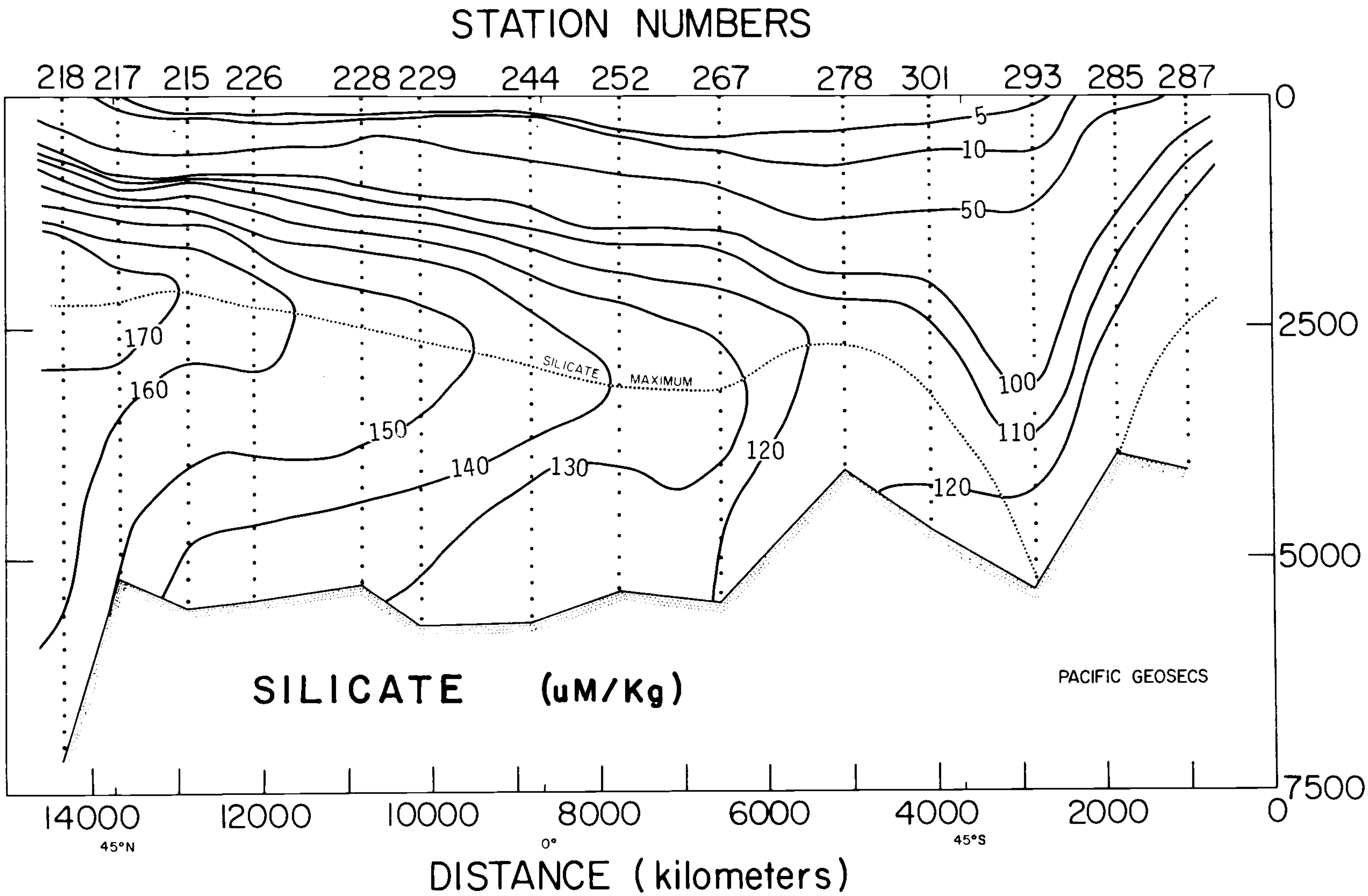

FIGURE 4.1g PACIFIC OCEAN SECTION, SILICATE

marks the dividing zones between areas with a high concentration of silica in the surface layers and areas with a lower content of silica. This can be especially well observed by the relatively high surface values in southern latitudes (70° to 69°S). It can be related to the upward extension at those latitudes of the old returning waters from the North Pacific Ocean (Gordon, 1973; Reid et al., 1973).

In northern latitudes, beyond 44°N, high surface values of silicate content are also observed. These values are lower than those found in the southernmost latitudes of the Pacific. Ross (1974) relates the surface values of silicate in the North Pacific to upwelled waters south of the Aleutian Arc. These waters are younger than those that rise in the Antarctic divergence. Therefore, surface values of silicate content are lower at about 44°N than those about the Antarctic divergence. A slight increase in surface values is also observed near the Equatorial zone. It should also be noted that these surface values are related to the divergence zone shown by Reid (1965) at that latitude.

It is suggested by Ross (1974) that the low values observed in the surface central water masses are due to biological extraction and to the presence of a stable thermocline typical for all biologically active compounds in this area. This is strongly observed in the southern Pacific where the old surface waters are drifting south to rejoin the circum-Antarctic current system.

Generally, the high content of silicate contributes to intensive development of diatoms in the surface layer. As a result, a general decrease in silicate near the surface prevails until the summer thermocline disappears. Specifically, it is at the beginning of the fall-winter convection that increases occur in the surface silicate content. Below the euphotic zone, the rapid post-mortem dissolution of siliceous tests and advective processes cause a silicate increase to occur. This results in a strong increase at mid-depths and ultimately creates the high concentration of the silicate maximum seen in the Pacific. Ross (1974) suggests that at least 90% of the silicate tests formed in the ocean will never be preserved in the geologic record and most redissolve at the ocean bottom or in the water column.

The Pacific Ocean shows a south to north increase in concentration of dissolved silicate (Fig. 4.1g). This increase is observed at any level but is particularly clear in deep waters. This distribution is internally consistent with that of other parameters along the same section (Figs. 4.1d, e, f, and h). Also, this pattern mirrors the extension of the deep water into the Pacific Ocean suggested earlier (Reid, 1965). In the Pacific Ocean, the deep and bottom waters extend chronologically from south to north with the North Pacific Deep Waters being the oldest. These waters are farthest from their last contact with the photic zone and contain the highest silicate concentration.

A silicate maximum at intermediate depths is observed in the section. The intermediate maximum in the North Pacific is shallower and higher in silicate values than the maximum in the South Pacific. The depth of the intermediate maximum is not clearly related to the depth of the intermediate waters in the Pacific Ocean. Its origin can be explained neither by the effects of temperature and pressure nor by the solubility of silicate. It is suggested by Ross (1974) that the decrease in solubility due to low temperature and the slight increase in solubility of silicate due to high pressure tends to cancel out. Therefore, the maximum may represent the "core" of southerly flowing deep water originating in the Bering Sea. South of 40°S, the depth of the maximum deepens and tends to be confused with a zone of relatively poor silicate content. This feature, when compared with the salinity distribution in the Pacific Ocean (Fig. 4.1b) coincides with the salinity maximum that marks the intrusion in the South Pacific of the Antarctic Bottom Waters. Further south, the silicate maximum is found at the ocean bottom, as the Antarctic Bottom Water with high silicate plus bottom dissolution of silica rich sediment places the maximum near the sea floor.

AOU:

The apparent oxygen utilization, AOU, at some Point X within the ocean is meant to represent the oxygen utilized since the water parcel left the surface. It is defined by:

$$AOU = O'_2 - O_2 \tag{4.1}$$

where O'_2 is the solubility of oxygen at the temperature T and salinity S and O_2 is the concentration of oxygen measured (Redfield et al., 1963). Therefore, the AOU distribution should be opposite to that for the oxygen (Fig. 4.1h).

The AOU in the Pacific increases from south to north in a similar pattern since the oxygen is decreased due to oxidation of organic matter. Surface waters of the Pacific Ocean are substantially

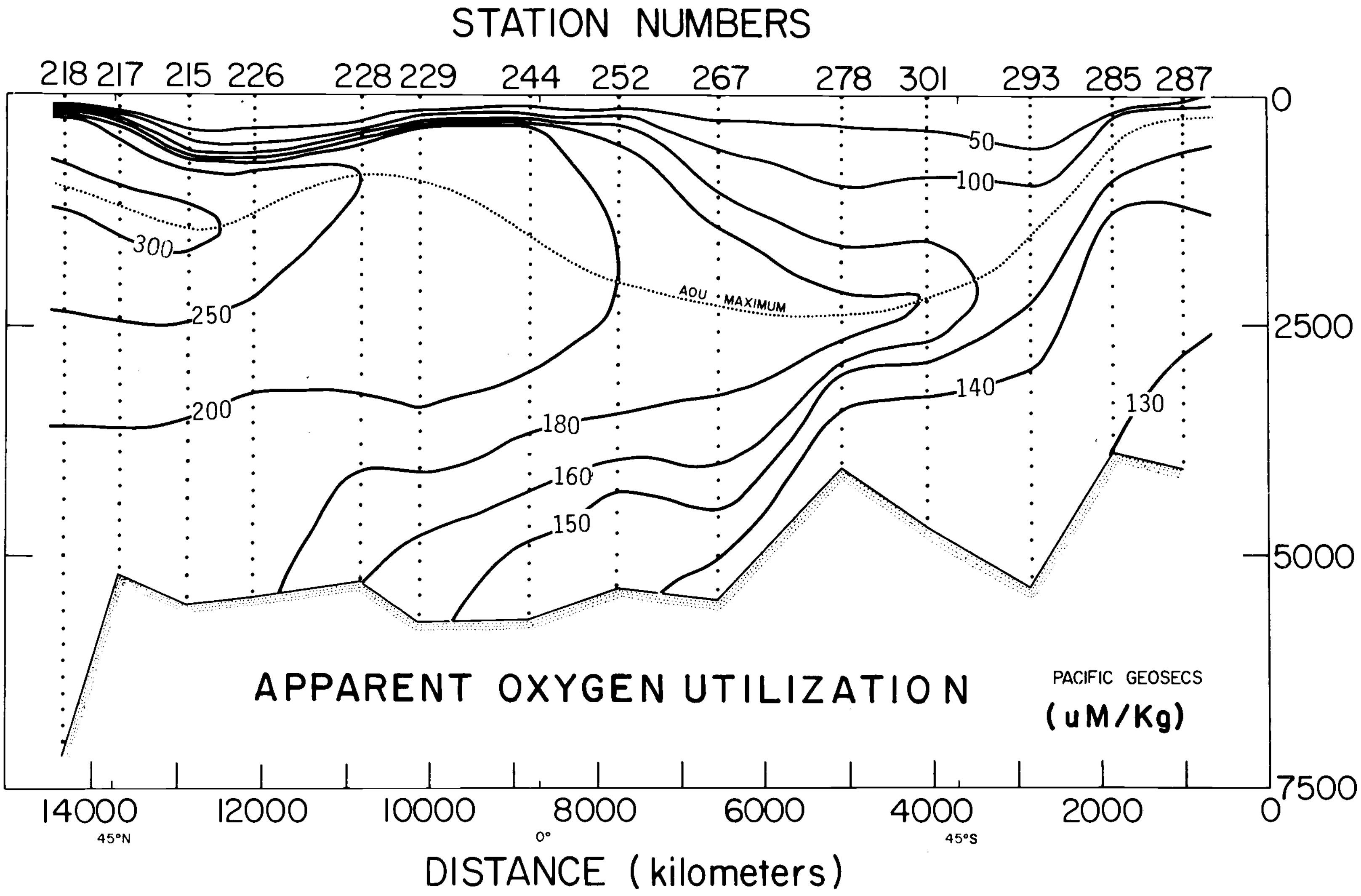

FIGURE 4.1h PACIFIC OCEAN SECTION, AOU

supersaturated through the section. Pytkowicz et al. (1966) suggest that supersaturation values can be due to strongly active photosynthesis, an increase in temperature, or both mechanisms combined. The data in the section was gathered during the summer months for both southern and northern hemispheres. Therefore, the data suggest that the high productivity of the Pacific Ocean overrides the effect of temperature on the AOU values.

At intermediate depths, the AOU maximum is situated near the oxygen minimum layer. It marks the transition zone between the intermediate waters rich in oxygen and the less oxyginated deep waters. A much stronger AOU minimum is seen in the North Pacific where the older water has undergone considerably more oxidation.

In the northeast Pacific Ocean, the AOU was utilized as a qualitative indicator of the water movement by Pytkowicz (1966). He states that AOU is a useful parameter since it permits a comparison of the relative utilization of oxygen at various points in the ocean and thus gives an indication of the direction of the water movement. An application of this method is shown in Figure 4.1h; it gives slowly increasing AOU values at the ocean bottom proceeding northward.

The AOU values for the Deep Pacific Waters show an increase from south to north suggesting, as has been long recognized (Knauss, 1962; Reid, 1965), that the deep waters move from the south to the North Pacific Ocean. Relatively low values of AOU in the South Pacific are correlated with the high oxygen water of Antarctic origin. These waters are younger than those in the North Pacific and correspond to the intrusion of Antarctic Bottom Waters into the South Pacific. The

AOU contour of 140 μM/kg has been used to define the Antarctic Bottom Water intrusion in the Pacific Ocean (Chung, 1975).

Preformed Phosphate and Nitrate:

According to Redfield et al. (1963), the total dissolved inorganic phosphate, $PO_{4(T)}$, is comprised of two parts: the preformed phosphate, $PO_{4(p)}$, brought from the surface source or sources, and the $PO_{4(ox)}$, the oxidative phosphate released since the waters left the surface by oxidation of organic matter. The same definition is applicable for nitrate. The preformed phosphate $PO_{4(p)}$ is a conservative property in the same sence as temperature and salinity because it is not affected by biological processes after the waters leave the surface but only by mixing. The same considerations are extended to preformed nitrate.

The preformed phosphate was studied in the Subarctic Pacific region by Sugiura (1965). He proposed the name "reserved" instead of "preformed" and defines the conservative part as the residual on subtracting the oxidative phosphate from the total in situ phosphate concentration. In addition, he presents a diagram which suggests that the conservative and oxidative parts are added in subsurface layers and brought up to the surface by divergence. At the surface, both parts become preformed or reserved, part of which is transferred back to the subsurface layer through vertical mixing and the other part is taken up by the biomass. The biomass in turn generates oxidative phosphate at the expense of dissolved oxygen when it decays.

The distribution of these two conservative parameters are shown in Figures 4.1i and j. Zones of high surface preformed phosphate content are observed in high latitudes and around the Equator in agreement with the diagram of Sugiura (1965) while Deep Pacific Waters show a rather homogeneous value of about 1.0 μM/kg. At intermediate depths in southern latitudes, a zone of preformed content is observed with the highest values, 1.20 μM/kg, for preformed phosphate. This zone may correspond to the returning intermediate waters suggested by Pytkowicz (1968). Below this zone, typical values for deep waters of about 1.10 μM/kg are observed. The Antarctic Bottom Water intrusion in the South Pacific Ocean is also suggested by the data. The values of preformed phosphate for the bottom waters are about 1.15-1.20 μM/kg and they extend northward to about 10°N before being obscured by the lower values of the Pacific Deep Water.

Preformed nitrates have been studied by Park (1966) at the Subarctic Boundary. There, as well as in the southern latitudes and about the Equator, the distribution shown in Figure 4.1j for surface waters conforms with the mechanisms proposed by Sugiura (1965), although the signature is not as clear as for preformed phosphate. This may be a result of the nitrate data not being as precise as the phosphate for the GEOSECS Pacific.

Finally, a zone of high preformed nitrate content appears at intermediate depths in southern latitudes. The correspondence of these high preformed nitrate values with the returning intermediate waters suggested by Pytkowicz (1968) is not so clear. The Deep Pacific Waters appear to be characterized by values of about 15.0 μM/kg.

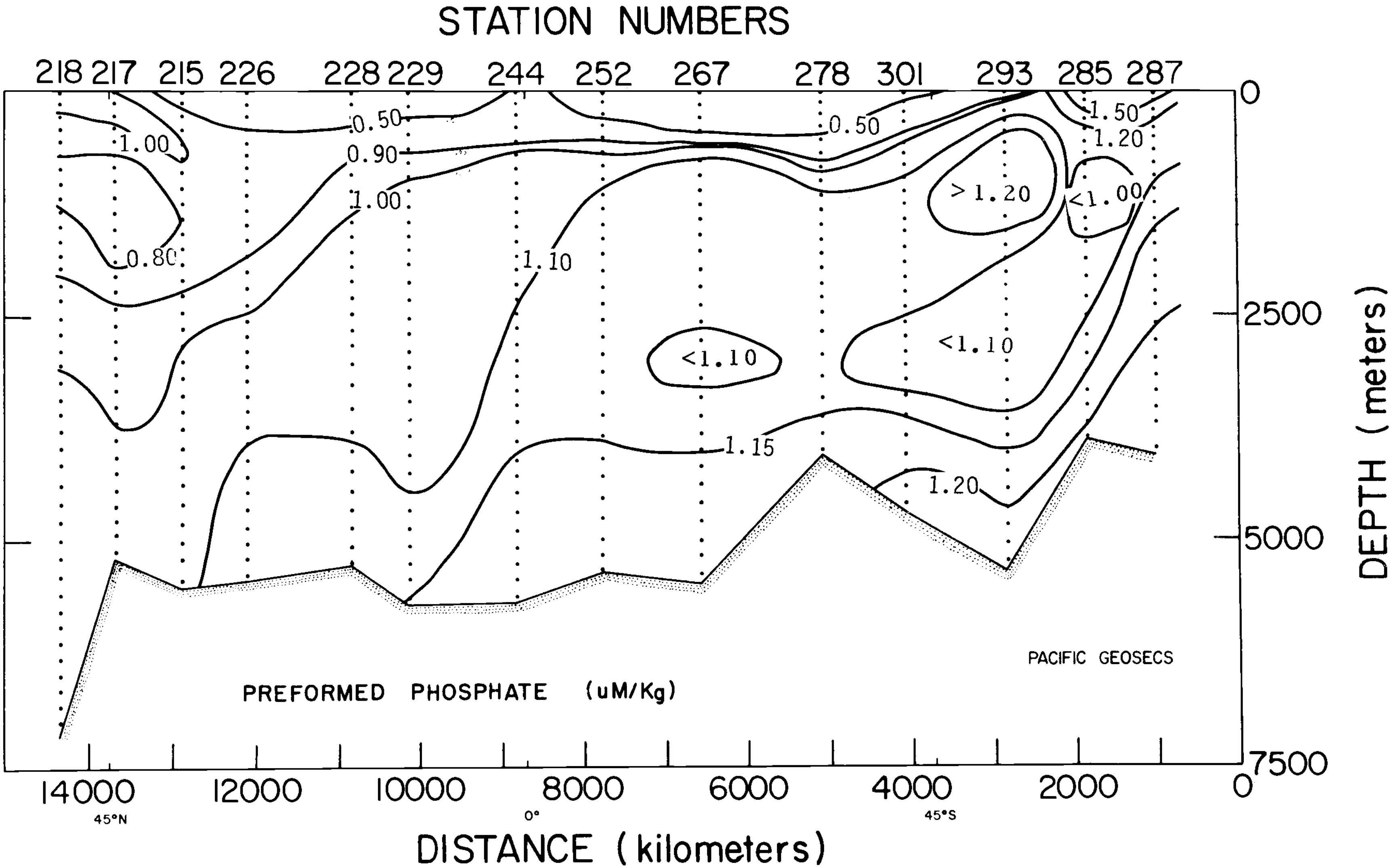

FIGURE 4.1i PACIFIC OCEAN SECTION, PREFORMED PHOSPHATE

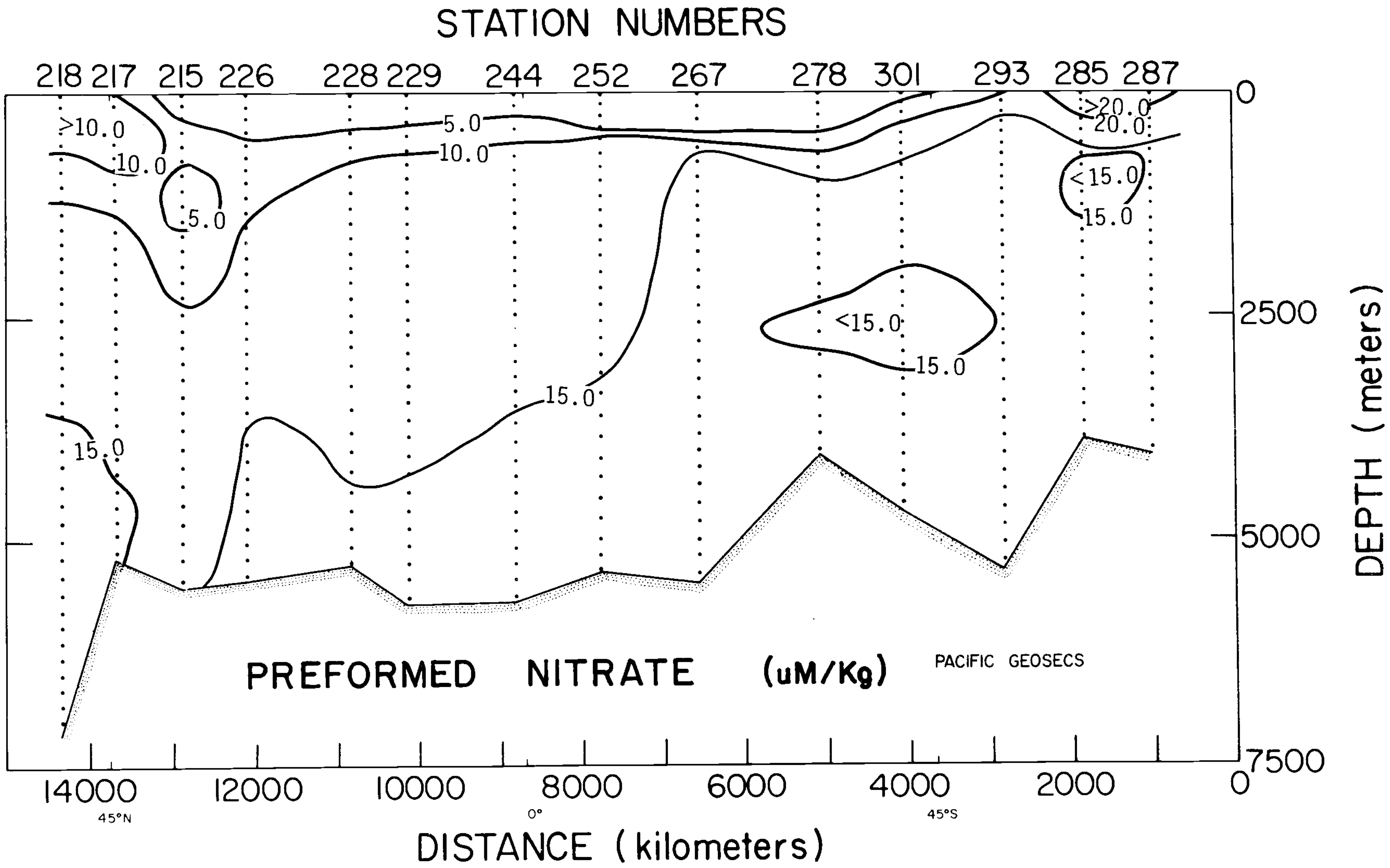

FIGURE 4.1j PACIFIC OCEAN SECTION, PREFORMED NITRATE

V. STABILITY

A stability analysis for each one of the stations in the GEOSECS Pacific section was performed. The purpose of this study was to look at the zones of stability maxima and minima and their possible correlation with the presence of different water masses.

It has been suggested by several authors (Wright, 1970; Reid and Lynn, 1971) that the presence of a zone of stability maxima in the water column may correspond with the transition layer between different water masses. In the same sense, low stability values are suggested to occur where more homogeneous conditions prevail within the water column. In addition, stability maxima are proposed (Reid et al., 1973) as layers of minimum motion between two water masses moving in opposite directions above and below the maximum. The quantity examined for stability is given by

$$E = \frac{\Delta'\sigma}{\Delta Z} \tag{5.1}$$

and the program used for this purpose is described in Appendix 2.

The quantity $\Delta'\sigma$ (g/cm^3) indicates the density difference that would exist between a pair of vertically adjacent samples if the deeper sample were moved adiabatically to the level of the upper sample (a distance ΔZ, in meters). It is assumed that an accuracy of about 10^{-6} g/cm^3 for the density calculation exists and an error of no more than 10^{-6} g/cm^3 is expected. In the deeper parts of the ocean, the vertical spacing observed in the data is of the order of 100-250 meters. The error in E is, therefore, about 1 to 2.5 x 10^{-8}

for the data observed in this interval.

Stability profiles were drawn for each one of the fourteen chosen stations. The changes in stability values throughout the water column were compared with inflection points in corresponding T-S diagrams and information taken from the section plots.

The northernmost stations (Figs. 5.1a, b, and c) show a well defined shallow stability layer. This layer of stability maximum becomes more intense and deeper toward mid-latitudes. The depth and intensity of the subsurface stability maximum is correlated with the pycnocline observed in mid-latitudes (Reid, 1965). Also, the lower stability values observed in subsurface water for the most northern stations may be associated with the formation of intermediate waters through the pycnocline (Reid, 1965). Below this stability maximum, other minor increments in stability values are observed in the station sequence 218, 217, 215, and 226 but in general a fairly homogenous condition prevails throughout the water column.

Station 218 (Fig. 5.1a) shows a slight increment in stability at about 140 meters depth, and a sudden decrease in stability below 500 meters depth. These changes in stability values appear to be well correlated with changes in the T-S diagram for this station. The data suggest that the upper increase in stability may be related to the position of the North Pacific Intermediate Waters. Also, the acute decrease in stability values at about 500 meters, and the low stability values from that depth to the bottom suggest a water mass of fairly homogeneous condition. This characteristic found in the Pacific Bottom Water has been discussed earlier.

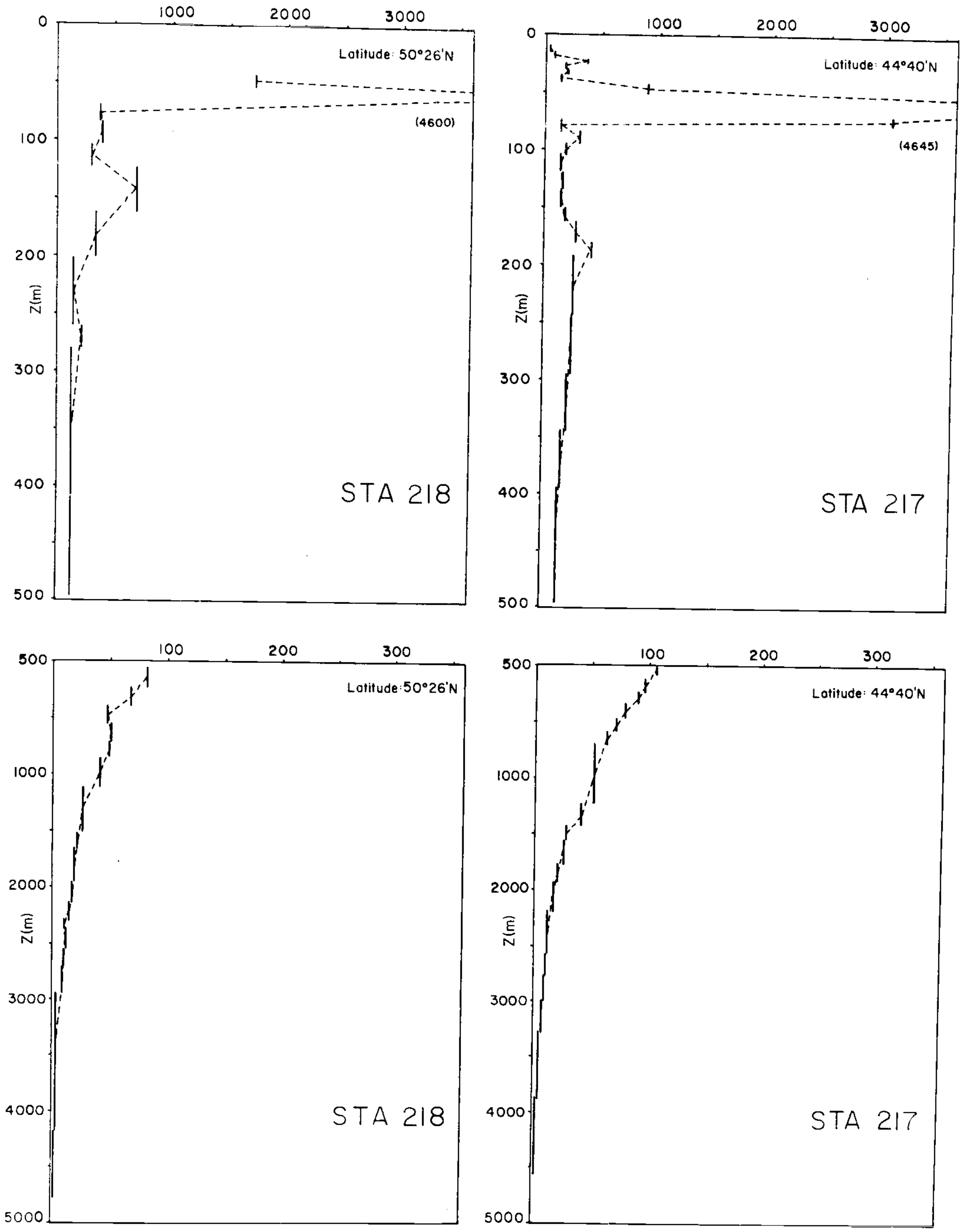

FIGURE 5.1a STABILITY CURVES IN THE NORTH PACIFIC ($X10^8$)

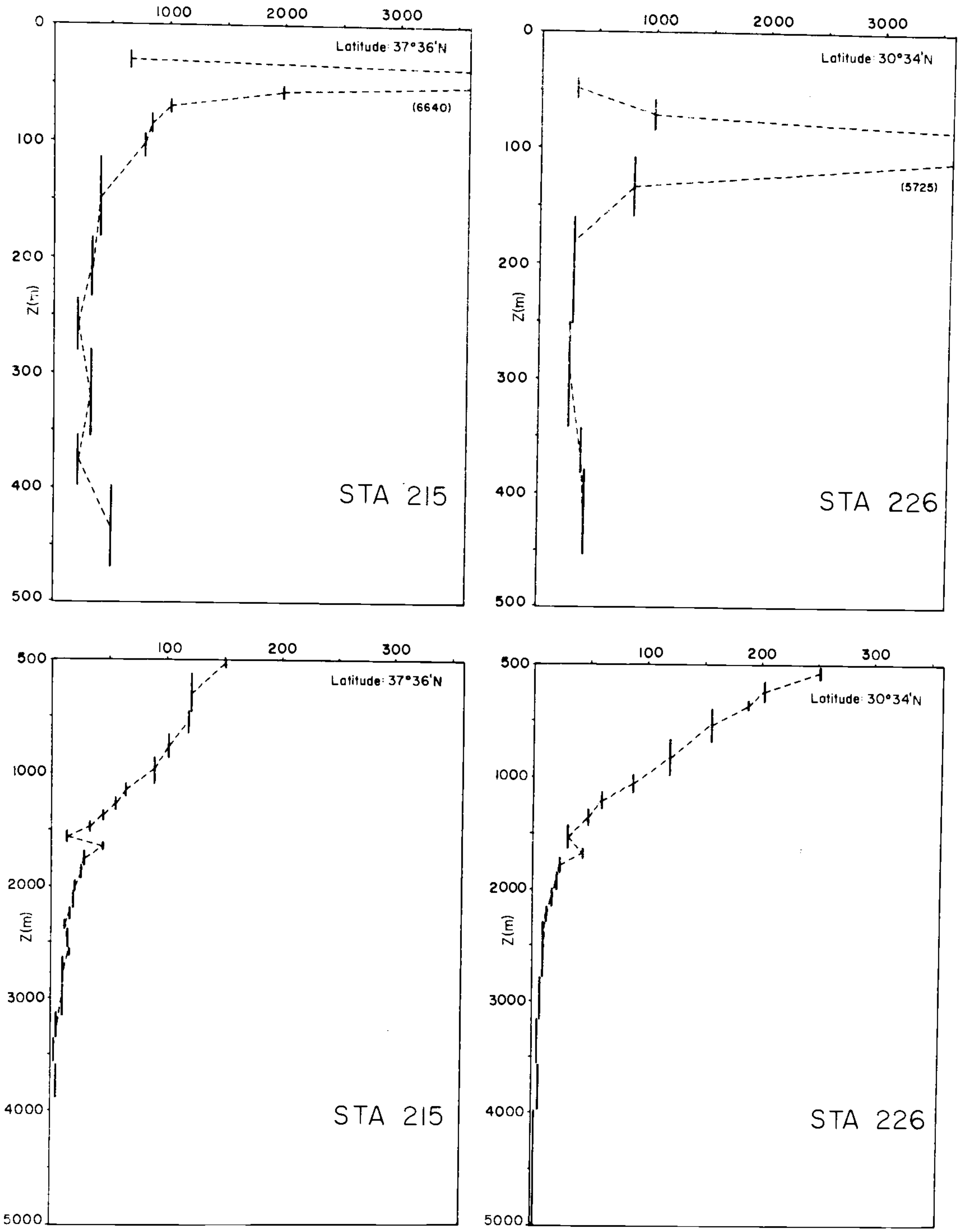

FIGURE 5.1b STABILITY CURVES IN THE NORTH PACIFIC $(X10^8)$

Stations 217, 215 and 226 basically show a similar stability distribution as does Station 218 (Figs. 5.1a and b). First, a strong shallow stability maximum that deepens toward lower latitudes is present at these stations. In addition, the data also show a slight increase in stability at a variable depth below the shallow maximum. Secondly, the minor maximum also deepens to some extent toward mid-latitudes until it reaches depths of about 420 meters at Station 226. Below this depth a sharp decrease in stability values is observed in these stations toward the bottom, suggesting the presence of homogeneous Pacific Bottom Waters.

Stability values throughout the water column from 19°N to 19°S are shown in Figures 5.1c and d. Some general remarks can be made for the section before looking at each one of the stations separately. First, at about 19°N, Station 228, the shallow stability maximum has decreased noticeably and is observed at about 100 meters depth. Near the Equator, Station 229 at 13°N (Fig. 5.1c), this maximum has again increased to attain values similar to those observed in mid-northern latitudes and has become deeper in the water column. Further south, at Station 244 close to the Equator at 1°N, the shallow maximum has again decreased in intensity and stands at about the same depth of 200 meters (Fig. 4.1d). South of the Equator, from about 8°S to 19°S, the shallow stability maximum gets stronger and shallower than the maximum at Station 244 (Fig. 4.1d).

The decrease in intensity of the stability maximum between 19°N and 12°N as well as the low stability values for this maximum noticed between 1°N and 8°S can be correlated with the divergence zones

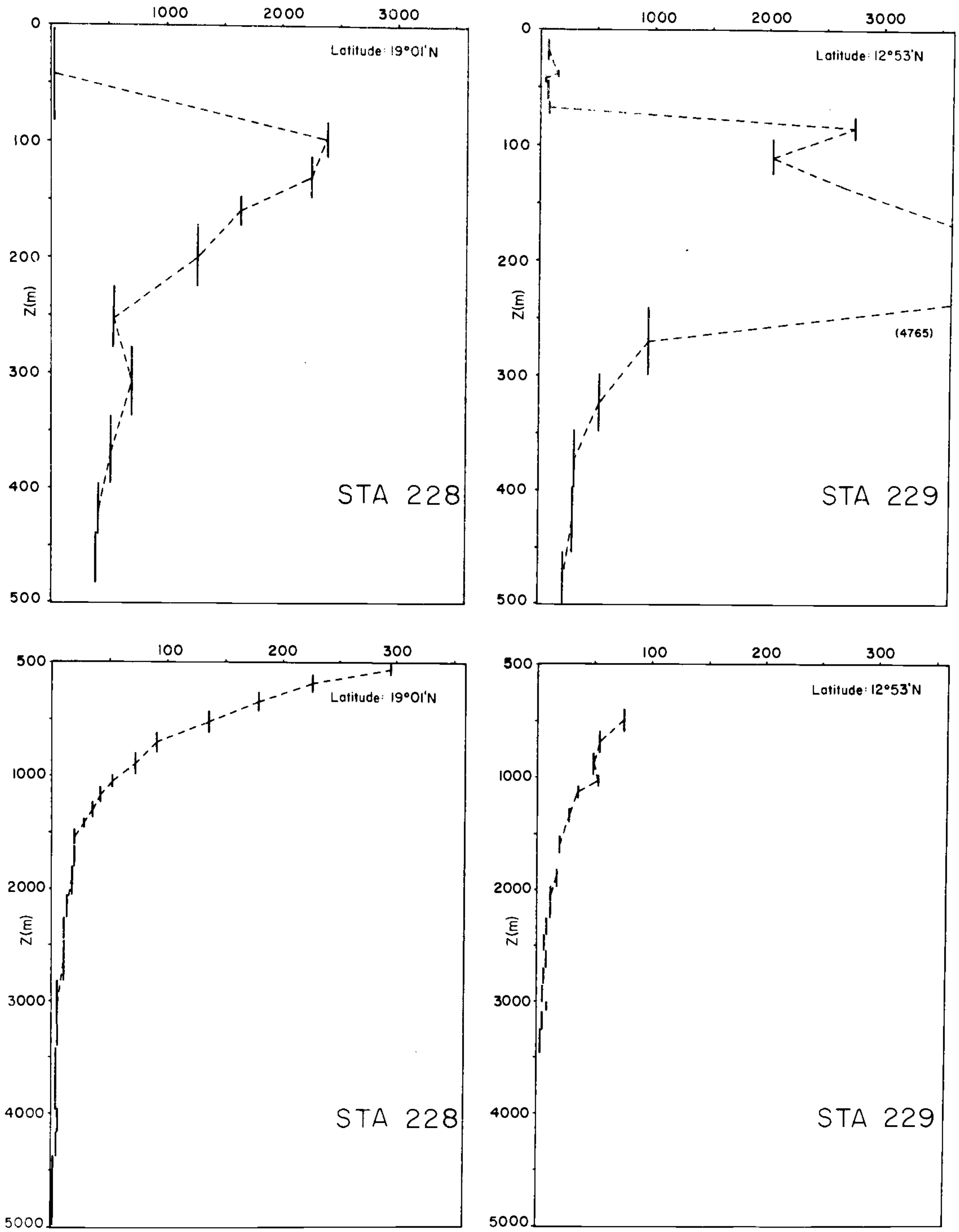

FIGURE 5.1c STABILITY CURVES IN THE NORTH PACIFIC $(\times 10^{8})$

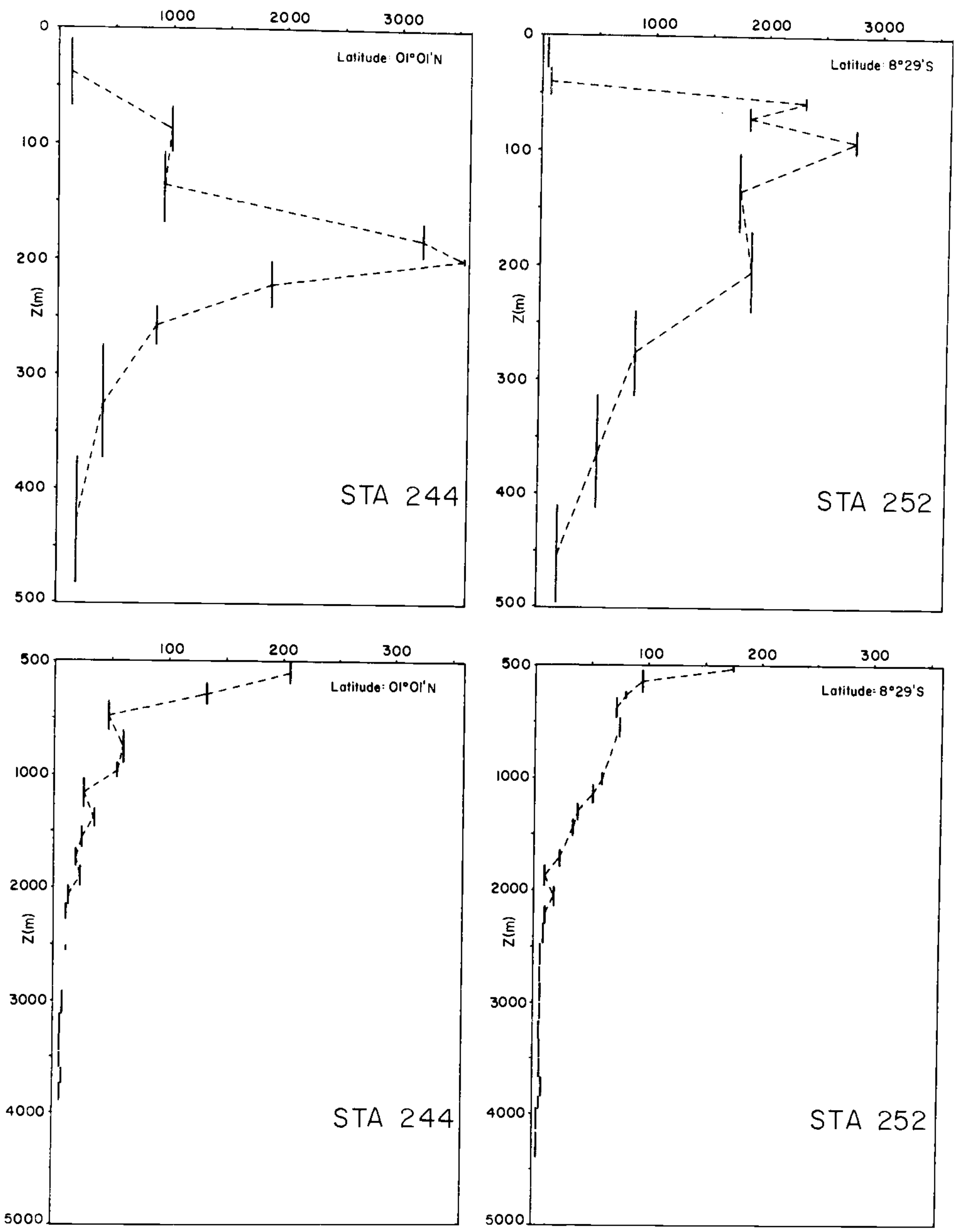

FIGURE 5.1d STABILITY CURVES IN THE NORTH AND SOUTH PACIFIC ($\times 10^8$)

mentioned by Sverdrup et al. (1948). He places these zones immediately south of the Equator and north of 10°N. Relatively high stability values at the Equator itself are associated with the strong thermocline present there (Masuzawa, 1975). North of 19°N and south of 19°S, the stability maximum observed is associated with the characteristic pycnocline of mid-latitudes.

Station 228 (Figs. 5.1c) shows a very slight increase in stability below the shallow maximum at about 300 meters depth. This minor maxima does not appear in any of the subsequent stations or it tends to be obscured by the strong decrease of stability values observed in the Station 228, 229, 244, 252, and 267. This decrease takes place from about 500 to 630 meters and tends to be deeper toward southern latitudes. Below this decrease in stability at each of the stations analyzed, the stability values does not change abruptly suggesting the presence of Pacific Bottom Waters. The stability values near the bottom at Stations 252 and 267 (Figs. 5.1d and e) does not show the Antarctic Bottom Water intrusion into the Pacific Ocean. This fact argues against the use of the term "benthic front" in this region as used by Craig (1972) and Chung (1975). A clear stability maximum such as between Antarctic Bottom Water and North Atlantic Deep Water is not apparent.

Stability values in the shallow maximum decrease to some extent from about 41°S to 61°S (Figs. 5.1e and f). Stability values for Station 293 were not plotted due to difficulties with the original data. Below the shallow maximum at Stations 301 and 285 (Figs. 5.1g and f) a small stability maximum is noticed through the water column

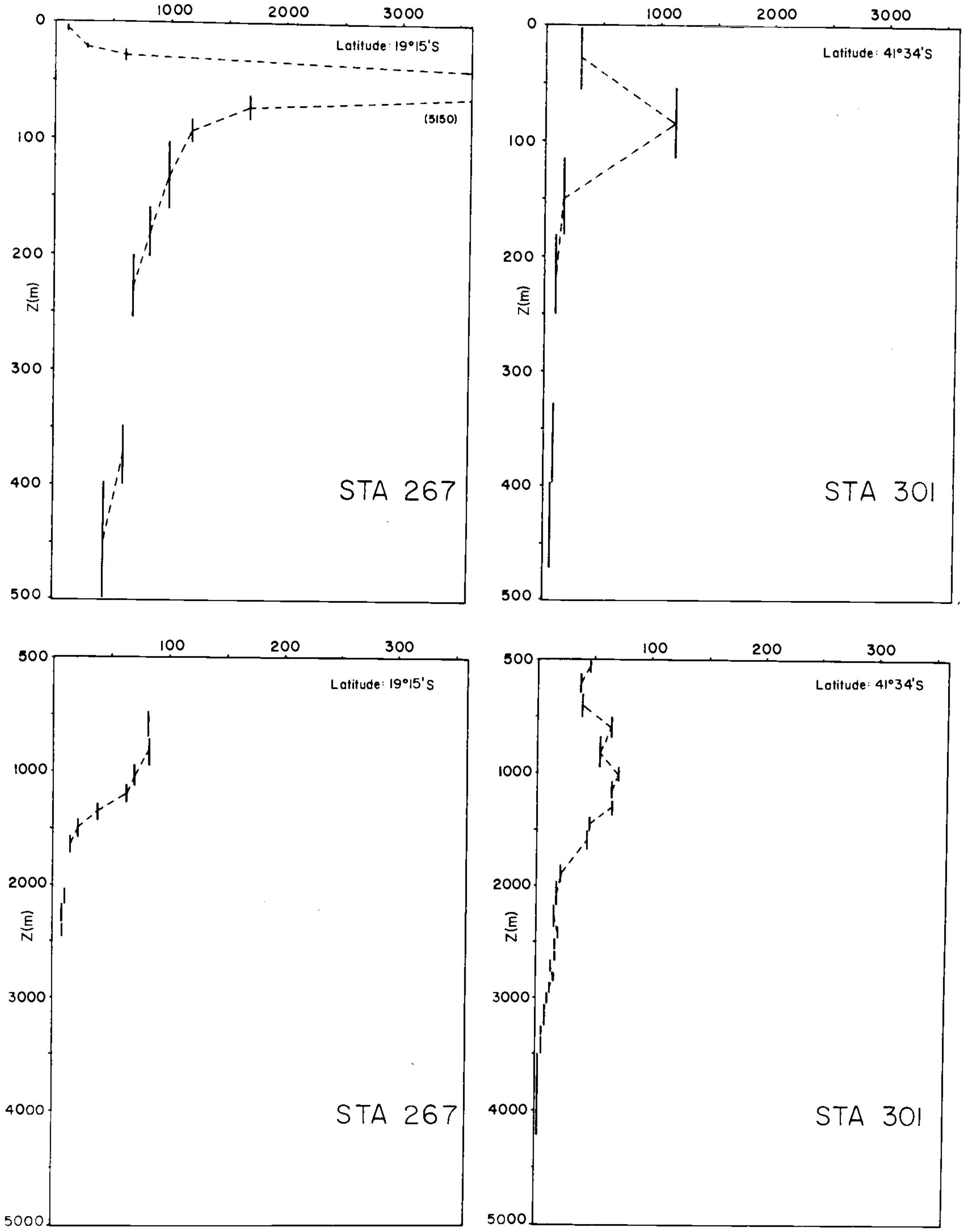

FIGURE 5.1e STABILITY CURVES IN THE SOUTH PACIFIC ($\times 10^8$)

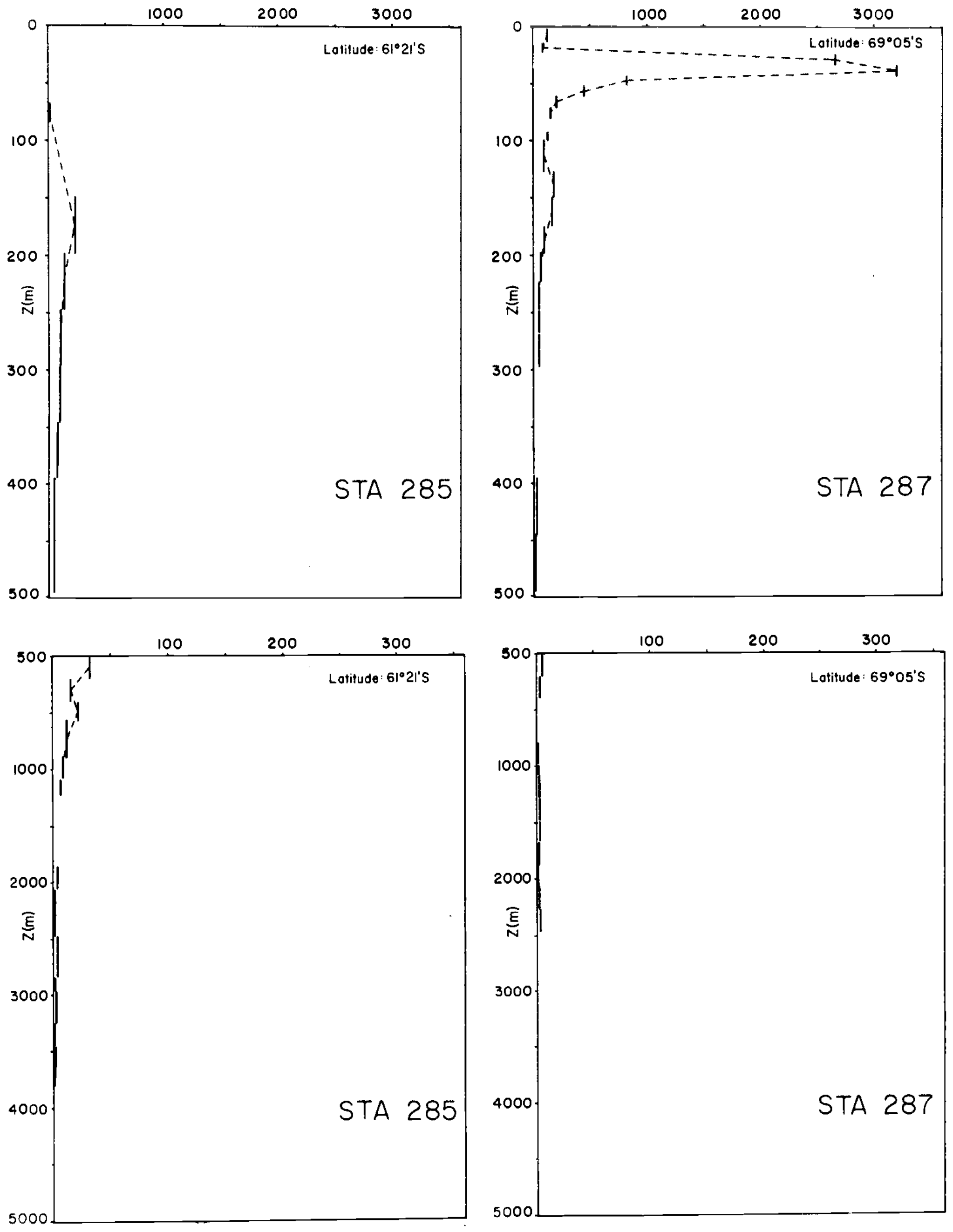

FIGURE 5.1f STABILITY CURVES IN THE SOUTH PACIFIC ($\times 10^8$)

at about 1000 meters depth. Below this feature, no other maximum is observed in the water column. A homogeneous bottom water appears to extend to the bottom and the separation of Antarctic Bottom Water from Pacific Deep Water is not suggested by the data at these latitudes.

The southernmost station (Fig. 5.1f) shows a strong and shallow stability layer. This maximum is associated with the presence of surface water of relatively low salinity (Fig. 4.1b). From there to the bottom, low stability values are present. This is expected as no great difference in density is found in Antarctic Waters.

In conclusion, the stability data for this GEOSECS Pacific section show some general features corresponding to the Intermediate and Pacific Bottom Water plus give information on the strength of the pycnocline at each station. Also, the "benthic front" of the South Pacific is not noticeably apparent from the stability field.

VI. CONCLUDING REMARKS

The data of the GEOSECS program for the Pacific Ocean alone comprises nine notebooks of information that can be used to construct a comprehensive picture of the dynamics of this ocean and its distribution of properties.

For future work, it would be advantageous to look into the several east-west crossings as well as the north to south transects so a new view of the Pacific Ocean can be obtained from the information contained in the GEOSECS program. The deep water circulation and the intermediate water extent as well as their property distributions can be understood much better in the North and South Pacific Oceans if all the Pacific GEOSECS sections are included in the data analysis. Also, some other regional features in the Pacific Ocean, such as the Antarctic Bottom Water intrusion into the Pacific Ocean, can be more clearly defined as to its northward and eastward extension in the South Pacific Ocean.

Although the methods for analysis of the data are many, three were chosen for this problem. The first involved finding a possible level of no motion as reference for a possible geostrophic transport from 50°N to 60°S. The depth of this level was found to be consonant with the oxygen minimum layer in mid-latitudes as earlier mentioned by Wyrtki (1961). Secondly, a set of plots for different parameters was prepared at about 180° on a north to south section. These plots provided an excellent illustration of Pacific circulation. Finally, a third approach centered around looking into the layers of stability maxima throughout the water column over the same section.

BIBLIOGRAPHY

Alvarez-Borrego, S. and K. Park. 1973. AOU as indicator of water-flow direction in the Central North Pacific. Journal of the Oceanographical Society of Japan. Vol. 27, 142-151.

Anderson, G. C., T. R. Parsons, and K. Stephens. 1969. Nitrate distribution in the Subarctic Northeast Pacific Ocean. Deep-Sea Res. Vol. 19, 329-334.

Atlas, E. L., L. I. Gordon, S. W. Hager, and P. K. Park. 1971. A practical manual for use of the Technicon AutoAnalyzer in seawater nutrient analysis. Technical Report 215, School of Oceanography, Oregon State University.

Bogoyaulenskiy, A. N. 1967. Distribution and migration of dissolved silica in oceans. Internat. Geology Rev. Vol. 9, 133-137.

Callahan, J. E. 1972. The structure and circulation of deep water in the Antarctic. Deep-Sea Res. Vol. 19, 563-575.

Callaway, J. C., R. D. Tomlinson, L. I. Gordon, and P. K. Park. 1973. An instruction manual for use of the Technicon AutoAnalyzer in precision seawater nutrient analyses. Manual for instruction of GEOSECS technicians. In Preparation. School of Oceanography, Oregon State Univ.

Carpenter, J. H. 1965. The Chesapeake Technique for the Winkler Dissolved Oxygen. Limnol. Oceanogr. Vol. 10, 141-143.

Chung, Y. 1975. Areal extent of the Benthic Front and variation of the scale height in Pacific Deep and Bottom Waters. J. Geophys. Res. Vol. 80 (30), 4169-4179.

Craig, H., Y. Chung, and M. Fiadero. 1972. A Benthic Front in the South Pacific. Earth Planet. Sci. Lett. Vol. 16, 50-65.

Cromwell, T. 1953. Circulation in a meridional plane in the Central Equatorial Pacific. J. Mar. Res. Vol. 12, 196-213.

Deacon, G. E. R. 1937. The hydrology of the southern ocean. Discovery Reps. Vol. 15, 1-124.

Deacon, G. E. R. 1963. The southern ocean. In: The sea, edited by M. N. Hill, Interscience, New York, Vol. 2, 281-296.

Defant, A. 1941. Physical oceanography. Vol. 1 (1961), 492-497.

Dodimead, A. J., F. Favorite, and T. Hirano. 1963. Salmon of the North Pacific Ocean. Part II. Review of the oceanography of the Subarctic Pacific region. International North Pacific Fisheries Commission. Bulletin No. 13, 195 p.

Gilbert, W., W. Pawley, and K. Park. 1968. Carpenter's oxygen solubility tables and nomograph for seawater as a function of temperature and salinity. Corvallis, Oregon, Oregon State University, Department of Oceanography. 139 p. (Data Report No. 29).

Gordon, A. 1973. General ocean circulation. Proc. Symp. Numerical.

Hager, S. W., E. L. Atlas, L. I. Gordon, A. W. Mantyla, and P. K. Park. 1972. A comparison at sea of manual and AutoAnalyzer analysis of phosphate, nitrate, and silicate. Limnol. Oceanogr. Vol. 7 (10), 931-937.

Heath, G. R. 1974. Dissolved silica and deep-sea sediments: In Studies' in paleo-oceanography. Society of Economic Paleontologist and Mineralogists. Special Publication No. 20.

International Southern Ocean Studies (ISOS). 1974. Southern Ocean Workbook. A collection of reprints on southern ocean dynamics. Two volumes.

Johnson, R. E. 1972. Antarctic Intermediate Waters in the South Pacific Ocean. Doctoral dissertation. Corvallis, Oregon State University. 170 numb. leaves.

Knauss, J. 1960. Measurements of the Cromwell Current. Deep-Sea Res. Vol. 6, 265-286.

Knauss, J. A. 1962. On some aspects of the deep circulation of the Pacific. J. Geophys. Res. Vol. 67 (10), 3943-3954.

Knauss, J. 1971. Equatorial current systems in the sea. Edited by M. N. Hill, Interscience, New York, Vol. 2, 235-251.

Kozlova, O. G. 1962. Diatomageous algae in suspension and in the bottom deposits of the southern part of the Indian and Pacific Oceans. Master's thesis. Inst. of Oceanology, A.S. U.S.S.R., 1963.

Masuzawa, J. 1963. Flux and water characteristics of the Pacific North Equatorial Current. Studies on oceanography. 121-128.

Masuzawa, J. and K. Nagasaka. 1975. The 137° oceanographic section. J. Marine Res. Supplement. 109-116.

Montgomery, R. B. 1954. Analysis of a Hugh M. Smith oceanographic section from Honolulu southward across the Equator. Jour. Mar. Res. Vol. 13, 67-75.

Newman, G. and W. J. Pierson, Jr. 1966. Principles of physical oceanography. Edited by Prentice-Hall, Inc. 494-500 pp.

The Pacific Ocean, Vol. 3. Chemistry of the Pacific Ocean. The Academy of Sciences of the U.S.S.R. Institute of Oceanology. 1966. Processed for Defense Documentation Center. Defense Supply Agelry.

Park, K. 1966. Deep-Sea pH science. Vol. 154, 1540-1542.

Park, K. 1967. Chemical features of the Subarctic Boundary near 170°W. J. of the Fish. Res. Board of Canada. Vol. 24, 899-908.

Pytkowicz, R. M. and D. R. Kester. 1966. Oxygen and phosphate as indicators for the deep intermediate waters in the Northeast Pacific Ocean. Deep-Sea Res., Vol. 13, 373-379.

Pytkowicz, R. M. 1968. Water masses and their properties at 160°W in the southern ocean. J. Oceanogr. Soc. of Japan. Vol. 24 (1), 21-31.

Redfield, A. C. B. H. Ketchum, and F. A. Richards. 1963. The influence of organisms on the composition of seawater. In: The Sea, ed. by M. N. Hill, Vol. 2, New York, Interscience, 26-77.

Reed, R. K. 1969. Deep water properties and flow in the Central North Pacific. J. Mar. Res.

Reid, R. O. 1948. The Equatorial Currents of the Eastern Pacific as maintained by the stress of the wind. J. Mar. Res. Vol. 7, 74-99.

Reid, J. L., Jr. 1962. On circulation, phosphate-phosphorus content, and zooplankton volumes in the upper part of the Pacific Ocean.

Reid, J. L., Jr. 1965. Intermediate waters of the Pacific Ocean. Johns Hopkins Oceanogr. Stud., No. 2, 85 p.

Reid, J. L. 1969. Preliminary results of measurements of deep currents in the Pacific Ocean. Nature, Vol. 221, 848.

Reid, J. L. and R. J. Lynn. 1971. On the influence of the Norwegian-Greenland and Weddell Seas upon the bottom waters of the Indian and Pacific Oceans. Deep-Sea Res. Vol. 18, 1062-1088.

Reid, J. L. 1973. The shallow salinity minima of the Pacific Ocean. Deep-Sea Res. Vol. 20, 51-68.

Reid, J. L., Jr. and P. L. Lonsdale. 1973. On the flow of water through the Samoan Passage. J. Phys. Oceanogr. Vol. 4, 58-73.

Stommel, H. The abyssal circulation. Deep-Sea Res. Vol. 5 (1), 80-82.

Stommel, H. and A. B. Arons. 1960. On the abyssal circulation of world oceans - I. Stationary Planetary Flow Patterns on a Sphere. Deep-Sea Res. Vol. 6, 140-154.

Stommel, H. and A. B. Arons. 1960. On the abyssal circulation of world ocean - II.

Stommel, H. 1964. Summary charts of the mean dynamic typography and current field at the surface of the ocean, and related functions of the mean wind stress. Studies of Oceanogr. 53-58.

Sugiura, Y. 1965. Distribution of reserved (preformed) phosphate in the Subarctic Pacific region. Papers in Meteorology and Geophysics, Vol. 15, 208-215.

Sverdrup, H. V., M. W. Johnson, and R. H. Fleming. 1942. The oceans, their physics, chemistry, and general biologia. New York, Prentice-Hall, 1089 p.

Taft, A. B. 1963. Distribution of salinity and dissolved oxygen on surface of uniform potential specific volume in the South Atlantic, South Pacific and Indian Oceans. J. Mar. Res. Vol. 21 (2), 129-140.

Tully, J. P. and A. J. Dodimead. 1957. Canadian oceanographic research in the northeast Pacific Ocean. M.S. Report, Fisheries Research Board of Canada. Pacific Oceanographic Group. 11 p.

Uda, M. 1963. Oceanography of the Subarctic Pacific Ocean. Journal of the Fisheries Research Board of Canada. Vol. 20, 79-119.

Warren, B. A. 1971. Antarctic Deep Water contribution to the world ocean. Research in the Antarctic. American Association for the Advancement of Science. 631-643.

Warren, B. A. 1973. Transpacific hydrographic sections at lats. 43°S and 28°S: the Scorpio Expedition - II deep water. Deep-Sea Res. Vol. 20, 9-38.

Weyl, P. K. 1965. On the oxygen supply of the Deep Pacific Ocean. Dep. of Oceanogr. Oregon State University. 215-219.

Wooster, W. S. and T. Cromwell. 1958. An oceanographic description of the Eastern Tropical Pacific. Bull. Scripps Inst. of Oceanogr. Univ. of Calif. Vol. 7, 169-282.

Wooster, W. S. and G. H. Volkman. 1960. Indications of the Deep Pacific circulation from the distribution of properties at five kilometers. J. Geophys. Res. Vol. 65 (4), 1239-1249.

Wright, W. R. 1970. Northward transport of Antarctic Bottom Water in the Western Atlantic Ocean. Deep-Sea Res. Vol. 17, 367-371.

Wust, G. 1936. Oberflachensalzgehalt, verdunstung und niederschlag auf dem weltmeer. Landenkundl forschung. Festschr. N. Krebs, Stuttgart.

Wyrtki, K. 1962. The oxygen minima in relation to ocean circulation. Deep-Sea Res. Vol. 9, 11-23.

Wyrtki, K. 1974. Sea level and the seasonal fluctuations of the Equatorial Currents in the Western Pacific Ocean. J. Phy. Oceanogr. Vol. 4, 91-103.

APPENDICES

APPENDIX I

```
      PROGRAM DYNM
      DIMENSION Z(24),D(2,24),DIF(24),LAT(2,2),STAT(2,2)
      READ LAT
      READ(3,50) LAT(1,1),LAT(1,2),STAT(1,1),STAT(1,2)
50    FORMAT(F3.0,F5.1,8X,2A8)
      READ(1,51) READ(1,51)(Z(I),D(1,I),I=1,24)
51    FORMAT(33X,F8.0,29X,F7.3)
      I1=1
      I2=2
      READ(3,50) LAT(I2,1),LAT(I2,2),STAT(I2,1),STAT(I2,2)
      READ(1,70)(D(I2,I),I=1,24)
70    FORMAT(70X,F7.3)
      DO 5 I=1,24
      DIF(I)=D(I1,I)-D(I2,I)
 5    CONTINUE
      T=Q-0.0
      K=10.0/SIN(0.01745*(LAT(I1,1)+LAT(I2,1)+(LAT(I2,2)+LAT(I1-2))/60.0
     1)/2.0)/1.458E-4
      WRITE(61,52)STAT(I1,1),STAT(I1,2),LAT(I1,1),LAT(I1,2),STAT(I2,1)
     1STAT(I2,2),LAT(I2,1),LAT(I2,2)
52    FORMAT(1H1,/,2(20X,2A8,F10.0,F7.2,/)//)
     1STAT(I2,2),LAT(I2,1),LAT(I2,2)
      I=1
      WRITE(2,53)I,Z(I),D(I1,1),D(I2,I),DIF(I),Q,T
53    FORMAT(I10,F6.0,5F15.3)
      DO 7 I=2,24
      Q=(DIF(I)+DIF(I-1))*(Z(I)-Z(I-1))/2.0+Q
      T=-K*(Q-DIF(I)*Z(I))
      WRITE(2,53)I,Z(I),D(I1,I),D(I2,I),DIF(I),Q,T
 7    CONTINUE
      END
```

APPENDIX I - Flow Diagram

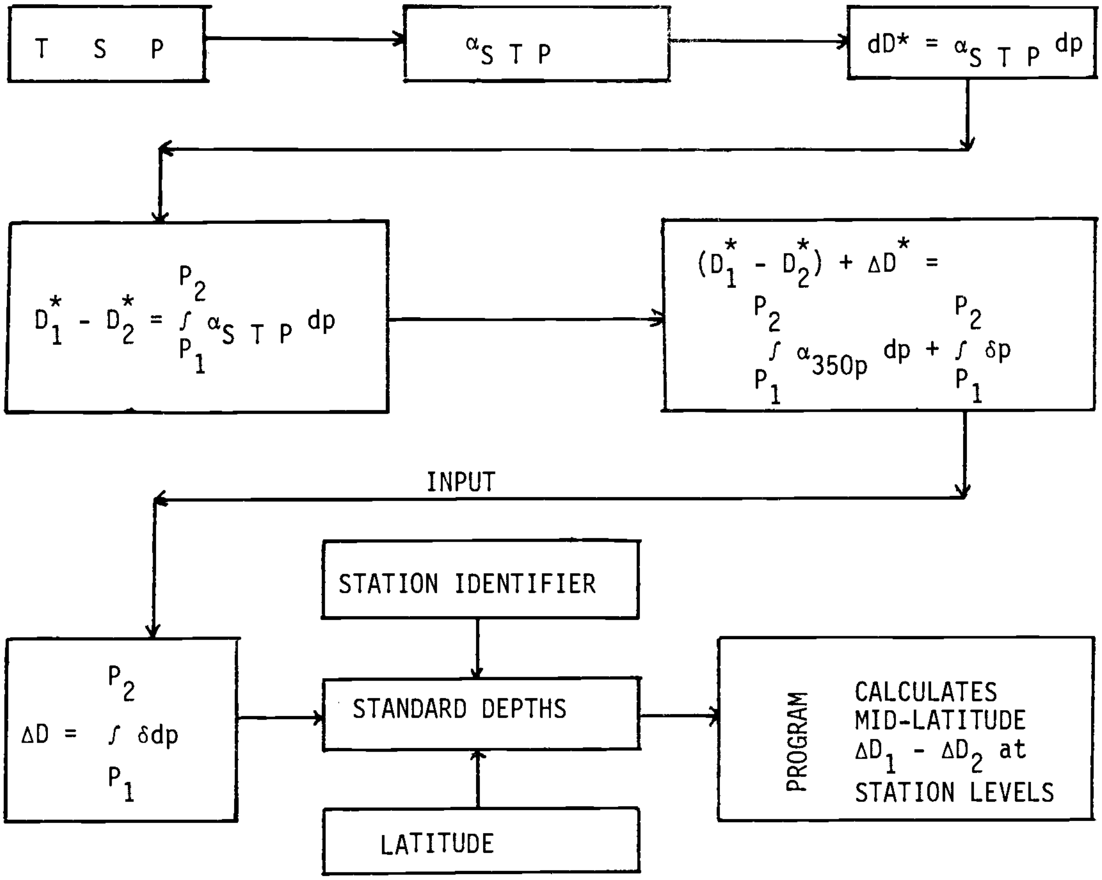

T = Temperature °C

S = Salinity S ‰

P = Pressure Decibals

α = Specific Volume

δ = Specific volume Anomaly

D^* = Dynamic Depth

P_2, P_1 = Standard Pressure Interval

This program was used in determining the level of no motion. The dynamic meters (ΔD) calculation was performed on the standard hydrographic data program used at OSU. This program then takes the station, identifier latitude, and dynamic meter standard depths as input. The program determines the mid-latitude and computes the difference of dynamic difference between successive stations for each standard depth.

APPENDIX II

```
      PROGRAM STB
      DIMENSION Z980),T(80),S(80),E(80),PT(80),SIGT(80),ID(5)
      E(1)=0.0
11    READ(1,2)ID
 2    FORMAT(5A2)
      IF(EOF (1)) GO TO 99
      READ (1,5)N
 5    FORMAT(I6)
      DO 10 I=1,N
      READ(1,15)Z(I),T(I),S(I)
15    FORMAT(3F10.0)
10    CONTINUE
      DO 12 K=1,N
      PT(K)=T(K) + 1.6E-5*Z(K) - 1.014E-5*Z(K)*T(K) + 1.27E-7*Z(K)
     1  *T(K)*T(K) - 2.7E-9*Z(K)*T(K)*T(K)*T(K) - 1.322E6*Z(K)*S(K) +
     2  2.62E-8*Z(K)*T(K)*S(K) - 4.1E-9*Z(K)*S(K)**2.0 - 9.14E-9
     3*Z(K)**2.0 + 2.77E-10*Z(K)**2.0*T(K) - 9.5E-13*Z(K)**2.0*T
     4(K)*T(K) + 1.557E-13*Z(K)**3.0
12    CONTINUE
      DO 16 L=1,N
16    SIGT(L)=SIGMAT(PT(L),S(L))
      DO 17 M=2,N
      P1=SIGT(M-1)*1.0E-3 + 1.0
      P2=SIGT(M)*1.0E-3 + 1.0
      DZ=Z(M)-Z(M-1)
17    E(M)=(P2-P1)/DZ
      WRITE(2,51)ID
51    FORMAT(10X,5A2)
      DO 40 J=1,N
      WRITE(2,25)Z(J),T(J),PT(J),S(J),SIGT(J),E(J)
25    FORMAT(F7.0,4F8.3,E15.5)
40    CONTINUE
      GO TO 11
99    STOP
      END
```

APPENDIX II - Flow Diagram

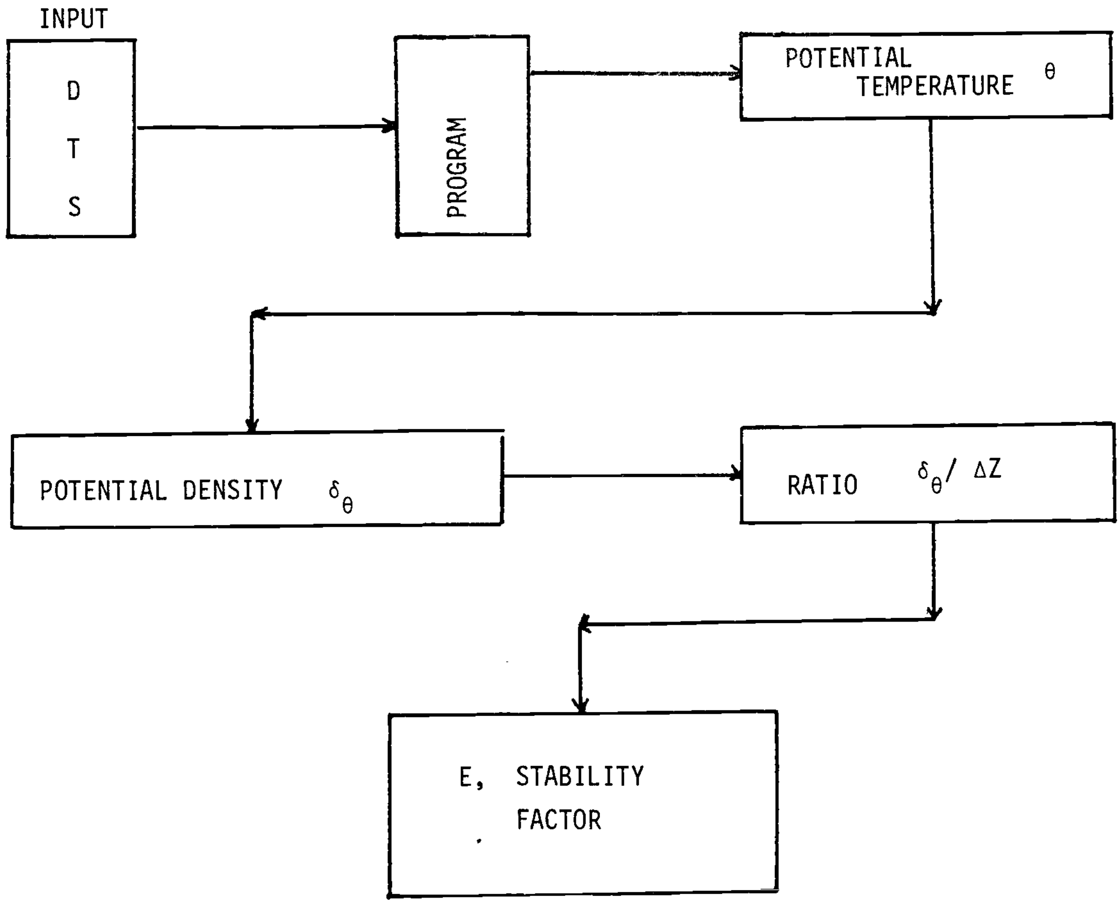

D = Depth (meters)

T = Temperature 7°C (in situ)

S = Salinity S ‰

The stability program computes the stability of a water parcel at a depth Z as if the water had been moved adiabatically to the surface. From this information a change in density with depth is calculated. The program requires in situ temperature, salinity, and depth information as input. The potential temperature and sigma theta (σ_θ) is then calculated along with the stability factor (E).